“ALEXANDRU IOAN CUZA” UNIVERSITY OF IASI

FACULTY OF CHEMISTRY
CHEMISTRY DOCTORAL SCHOOL

Development of analytical methods for the chemical characterization of primary bioaerosols from ambient particulate matter

SUMAR OF THE PHD THESIS

PhD supervisor,
Prof. PhD habil. **Cecilia ARSENE**

PhD Student,
Chemist **Cristina IANCU**

September 2025

Acknowledgments

First of all, I am deeply grateful to Professor PhD habil. Cecilia ARSENE, for her scientific vision, her kind yet demanding expectations, and her constant trust in guiding me throughout my doctoral journey. I am thankful for the time she dedicated to repeatedly reading each report, for her precise observations, and for the ethical standards she consistently demonstrated. Additionally, her support in facilitating access to research infrastructure, specialized collaborations, and encouraging the dissemination of results was essential for the completion of this academic endeavor. Without her guidance, rigor, and generosity, this thesis would not have achieved the coherence and consistency presented.

I would like to extend special thanks to the members of the guidance and academic integrity committee: Professor PhD habil. Romeo-Iulian OLARIU, Associate Professor PhD Iustinian-Gabriel BEJAN, Associate Professor PhD Naela COSTICĂ, and Professor PhD habil. Cezar Florin CATRINESCU. I thank them for their valuable advice, their support, their suggestions, and for the time they dedicated to my academic formation. I am grateful for their methodological observations, their constructive discussions, and for the continuous support throughout all stages of this research.

I would like to especially thank Dr. Cornelia NIȚĂ, CS Dr. Alina Giorgiana NEGRU, and CS Dr. Laurențiu Valentin ȘOROAGĂ, who were not just colleagues but also mentors, and who helped me immensely at each stage of my research. I thank CS Dr. Claudiu ROMAN, CS Dr. Tiberiu ROMAN, PhD student Ana – Maria RUSU (VASILACHE), and PhD student Ciprian MĂIREAN for their collegiality and the advice they offered.

I am deeply thankful to Miss CS III Dr. Gabriela MIHALACHE for her guidance and constant support in carrying out the initial microbiological investigations.

Warm thanks go to my family, friends, and especially to my mother, who never stopped believing in me when I had lost all hope. Their support has been one of the strongest anchors throughout these years.

I sincerely thank the RECENT AIR and CERNESIM Research Centers for providing the infrastructure needed for this research.

Contents

I. INTRODUCTION

Bioaerosols, or biological aerosols in the atmosphere, comprise a wide range of airborne fractions of biological origin (Manibusan and Mainelis, 2022). Bacteria, viruses, fungi and their fragments, as well as pollen grains, are recognised as biological agents with the potential to cause health problems worldwide (Haig et al., 2016; Buiarelli et al., 2019; Uddin et al., 2023; Xue et al., 2023). Primary biological aerosol particles (PBAPs) are solid aerosol particles of biological nature, with sizes ranging from approximately 10 nm to 100 µm (Gollakota et al., 2021). They include materials released by organisms in the form of spores, pollen, volatile organic metabolites, endotoxins, viable and non-viable microorganisms, as well as cellular fragments (Ferguson et al., 2019).

Scientific interest in bioaerosols dates back to the nineteenth century (**Figure 1**) and has increased markedly in recent decades, alongside the development of increasingly innovative measurement and analytical methods.

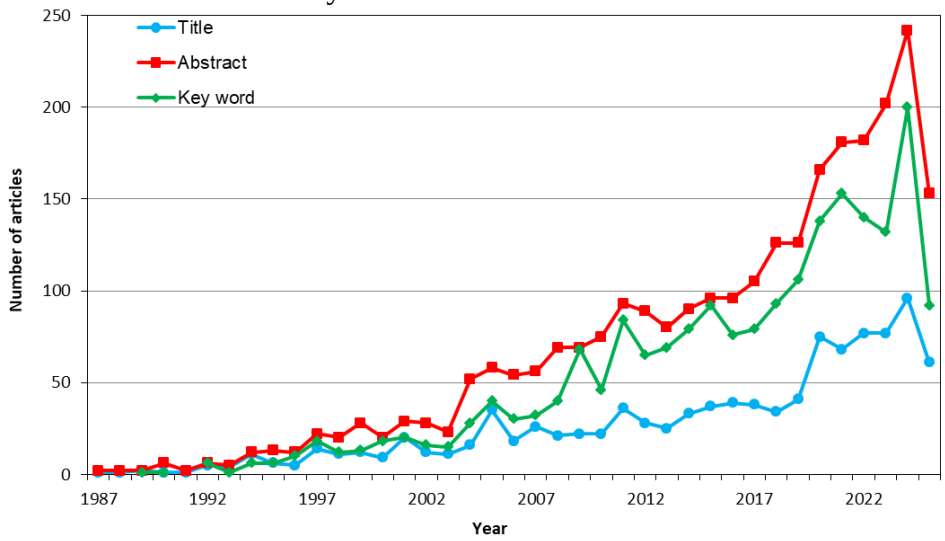

Figure 1: The annual variation in the number of articles containing the term "bioaerosol" in the title, abstract, or keywords (according to the Scopus database).

The objectives of the doctoral thesis were as follows:

- **Development and validation of optimised protocols** for the sampling and chemical characterisation of primary bioaerosols present in ambient particulate matter, in order to ensure analytical reproducibility and accuracy;
- **Comprehensive characterisation of particulate matter** in the urban area of Iasi, with a particular focus on **polycyclic aromatic hydrocarbons (PAHs)**, investigated as a potentially favourable matrix for the development and persistence of microbial communities;
- **Generation and integration of relevant information** on the biological component of atmospheric particles, contributing both to the enrichment of existing databases and to the development of a more comprehensive perspective on the role of bioaerosols in human health and environmental quality;
- **Identification and quantification of specific chemical compounds** (molecular biomarkers and chemical elements) associated with the biological fraction of atmospheric particulate matter (PM), aiming to define **chemically relevant signatures** for bioaerosol characterisation;
- **State-of-the-art assessment of the behaviour of selected markers** characteristic of microorganisms isolated from ambient particulate matter, tracking their dynamics throughout development-from inoculation to the mature stage.

PART II: ORIGINAL CONTRIBUTIONS

II.1 AMBIENT PARTICULATE MATTER IN THE URBAN AREA OF IASI AND THE CONTENT OF POLYCYCLIC AROMATIC HYDROCARBONS (PAHs) FROM A NEW PERSPECTIVE

II.1.1 Active sampling of aerosol particles by low-pressure impaction

Particulate matter samples were collected at the Air Quality Monitoring Station (AMOS) of "Alexandru Ioan Cuza" University of Iasi, located in the north-eastern part of the city, on the roof of the tallest university building (Building C), at ~35 m above ground level (47º9' N, 27º35' E). The site is representative of an urban receptor influenced by well-mixed air masses. The site configuration is illustrated in **Figure II.1.1**. A detailed characterisation of the measurement location has been provided in previous studies (Arsene et al., 2007, 2011; Galon-Negru et al., 2019).

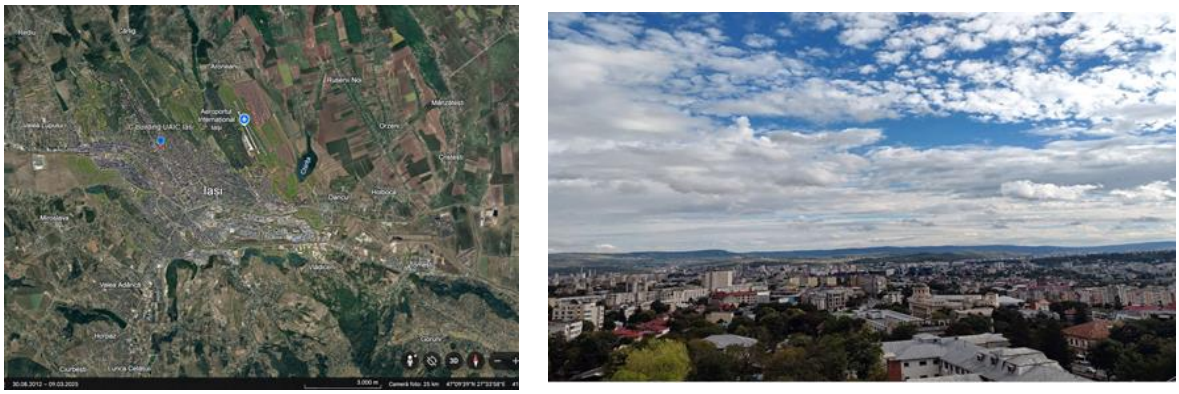

Figure II.1.1: Aerosol sampling site in Iasi, north-eastern Romania.

Active sampling of aerosol particles was performed using a low-pressure, cascade impactor-Dekati Low Pressure Impactor (DLPI)-operated at a flow rate of 30 L min^{-1}, as specified by the manufacturer. The device comprises 13 stages and size-segregates aerosols over the particle-size range 0.0276–9.94 µm. According to the calibration certificate, the 50% cut-point aerodynamic diameters were determined at 21.7 ºC, with an inlet pressure of 1013.3 mbar and an outlet pressure of 100 mbar. **Figure II.1.2** presents the sampling procedure steps and the aerodynamic diameters corresponding to each stage.

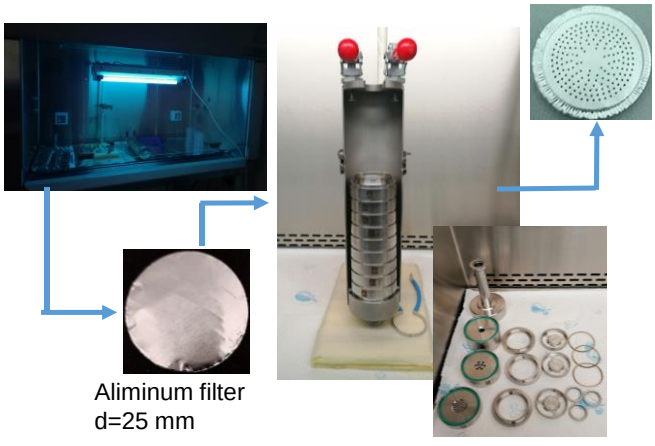

Stage number	D50% (µm)
1	0,0276
2	0,0556
3	0,0945
4	0,155
5	0,26
6	0,381
7	0,612
8	0,946
9	1,6
10	2,39
11	3,99
12	6,58
13	9,94

PM_{10} $PM_{2,5}$

Air Quality **Mo**nitoring **S**tation (AMOS)

Figure II.1.2: Key steps of the active aerosol particle sampling procedure using the Dekati Low Pressure Impactor (DLPI).

II.1.2 Determination of the mass concentrations of particulate matter collected in the urban area of Iasi

Table II.1.1 presents basic statistical parameters (mean, standard deviation, minimum, maximum) associated with the mass concentrations of the $PM_{2.5}$ and PM_{10} fractions collected over the period December 2015-April 2025; contributions made during the doctoral programme cover the interval April 2021-April 2025. All samples were collected using the DLPI impactor at the AMOS station during the time periods indicated.

Table II.1.1: Statistical parameters for the mass concentrations of the $PM_{2.5}$ and PM_{10} fractions collected using the DLPI impactor at the AMOS station.

a) Sampling period December 2015 – April 2025		
	Mass concentration $PM_{2,5}$ (µg m^{-3})	**Mass concentration PM_{10} (µg m^{-3})**
Average	15,0	16,5
Std. deviation	9,7	10,3
Minimum	0,6	0,6
Maximum	74,7	76,8
b) Sampling period April 2021 – April 2025		
	Mass concentration $PM_{2,5}$ (µg m^{-3})	**Mass concentration PM_{10} (µg m^{-3})**
Average	11,8	12,7
Std. deviation	8,0	8,5
Minimum	1,5	1,4
Maximum	52,1	55,4

The mass concentration distributions are shown in **Figure II.1.3**. Data for December 2015-March 2021 were provided by the research group involved in the doctoral programme. The estimated values are compared with the limit values set by Directive 2024/2881/EC: <10 µg m^{-3} for $PM_{2.5}$ and <20 µg m^{-3} for PM_{10}.

In **Figure II.1.3.a** (December 2015-May 2021), numerous episodes exceed the $PM_{2.5}$ limit value, with some reaching >40 µg m^{-3}.

Figure II.1.3.b includes the updated distributions through April 2025, highlighting the active sampling periods and the passive bioaerosol campaigns conducted in parallel with active sampling using the Dekati impactor.

(a)

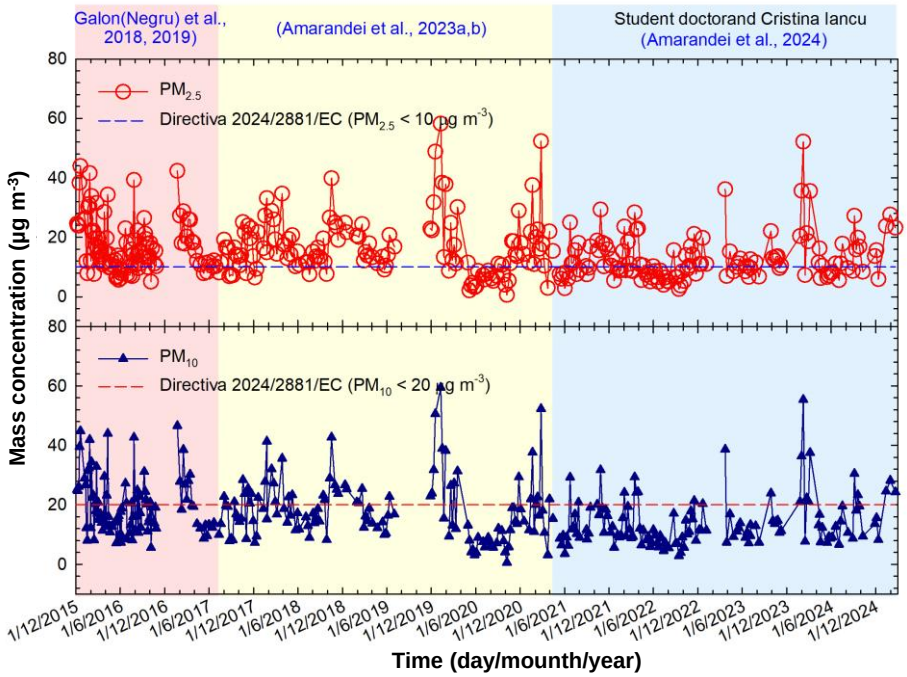

(b)

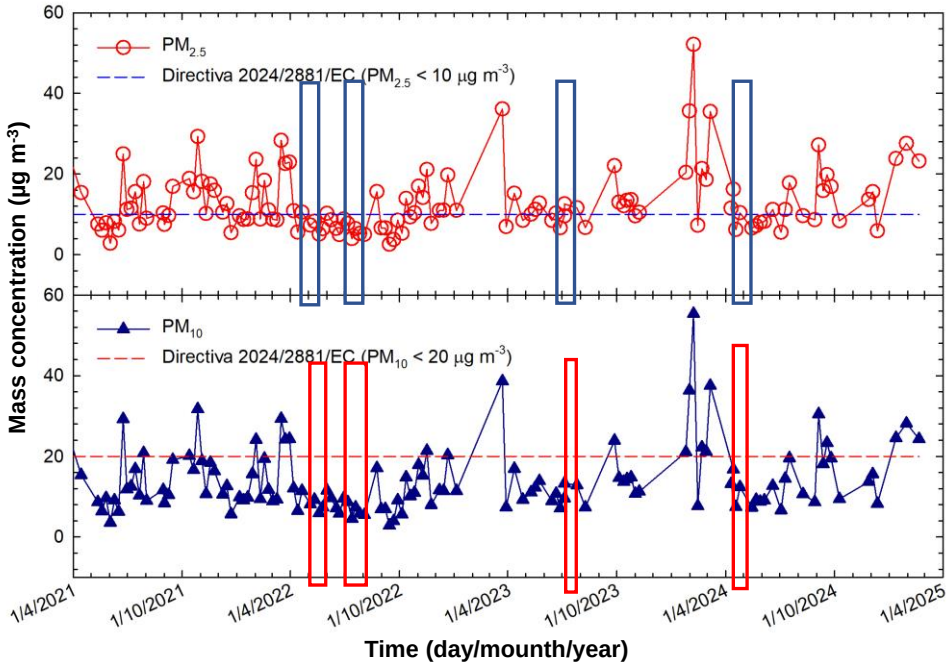

Figure II.1.3: Mass concentration of particulate matter collected during 2015-2024 **(a)**, and the averaged particulate matter mass concentration overlaid with bioaerosol particle sampling events **(b)**.

For the urban area of Iasi, the seasonal distributions of size-segregated aerosol particle mass concentrations are presented in **Figure II.1.4**.

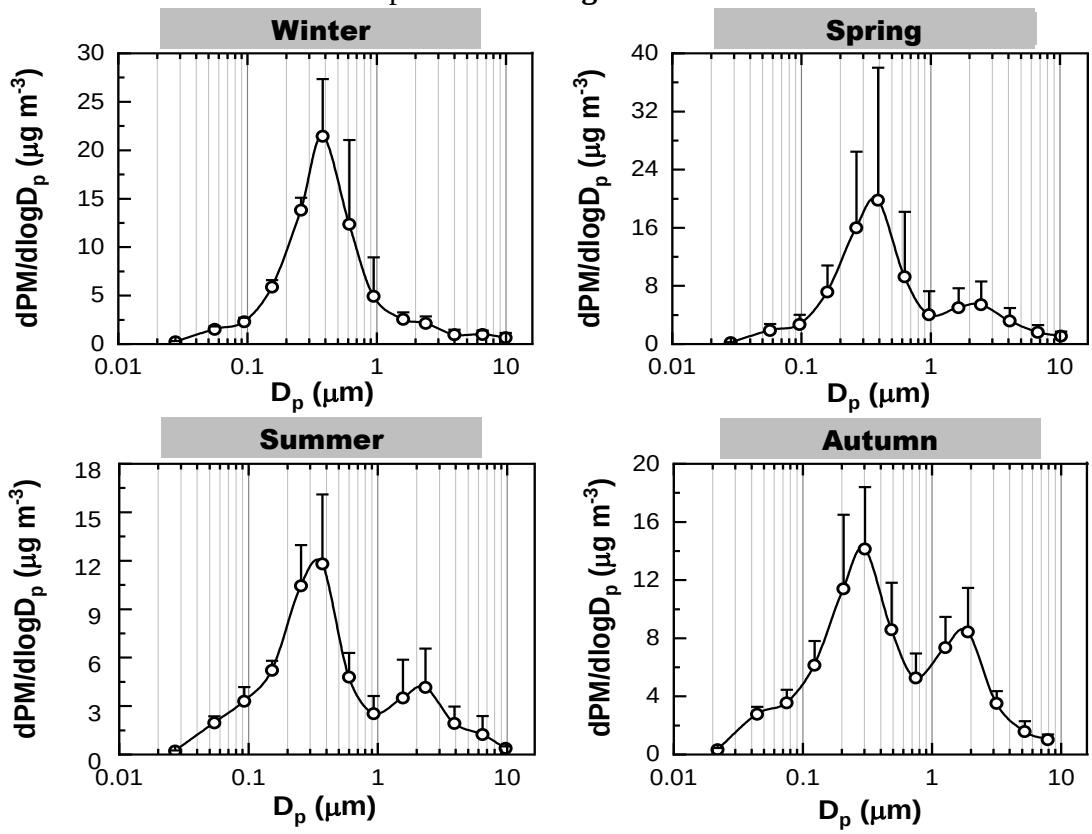

Figure II.1.4: Size-segregated (mean ± standard deviation) mass concentration distributions of particulate matter in the urban area of Iasi.

Figure II.1.4 shows a monomodal profile in winter and bimodal profiles in spring, summer, and autumn, with a dominant mode in the fine size range (381 nm) and a second mode in the coarse size range (2.39 μm). These distributions may be explained by the complex chemical composition of the particles.

II.1.3 Determination of PAH concentrations in ambient particulate matter from the urban area of Iasi, with potential implications for fungal–bacterial interactions within the potentially present bioaerosol fraction

PAHs in the urban particulate matter samples from Iasi were determined by UHPLC-FLD (Agilent 1290 Infinity UHPLC coupled to an Agilent 1260 Infinity FLD). Quantification was based on a mixed standard containing 18 PAHs at a concentration of 10 μg mL^{-1} in cyclohexane (Dr. Ehrenstorfer). For 17 PAHs, the abbreviations and molecular structures are presented in **Table II.1.2**.

Table II.1.2: Molecular structures of the PAHs analysed in aerosol samples from the urban area of Iasi.

PAHs	Abbreviation	Number of cycles	Structure
naphtalene	Nap	2	
1-methylnaphtalen	1MNap		
2- methylnaphtalen	2MNap		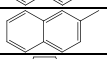
acenaphtene	Ace	3	
fluoren	Flu		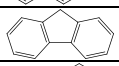
phenanthren	Phe		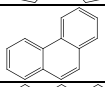
anthracen	Ant		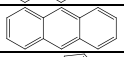
fluoranthen	Flt	4	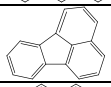
pyrene	Pyr		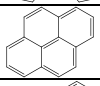
chrysene	Chr		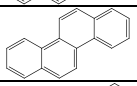
benzo[a]anthracen	BaA		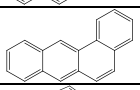
benzo[b]fluoranthen	BbF	5	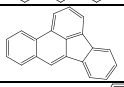
benzo[k]fluoranthen	BkF		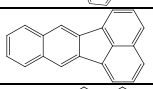
benzo[a]pyrene	BaP		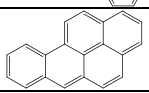
dibenzo[a,h]anthracen	DBA		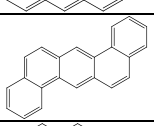
benzo[g,h,i]perylene	BghiP	6	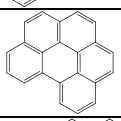
indeno[1,2,3-cd]pyrene	InP		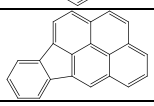

Figure II.1.5 depicts the key steps followed for PAH analysis using the UHPLC-FLD technique.

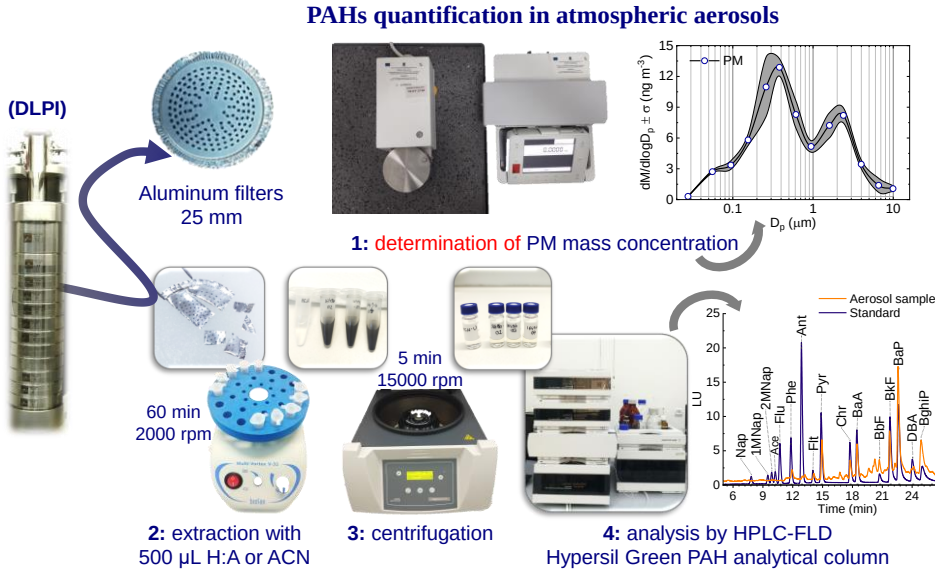

Figure II.1.5: Experimental steps involved in determining PM mass concentrations and PAH concentrations in atmospheric aerosols from the urban area of Iasi.

Figure II.1.6 presents the size-resolved mass concentration distributions for the analysed PAHs. The data shown in **Figure II.1.6** indicate a well-defined seasonal variability in concentrations associated with the aerosol fractions characterised by particle diameters Dp < 0.1 µm (**Figure II.1.6a**) and 0.1-1.0 µm (**Figure II.1.6b**), with lower concentrations during the warm season than during the cold season. For the particle-size fractions with Dp between 1.0 and 2.5 µm (**Figure II.1.6c**) and 2.5-10 µm (**Figure II.1.6d**), elevated PAH and particulate matter concentrations are observed during November-January and March.

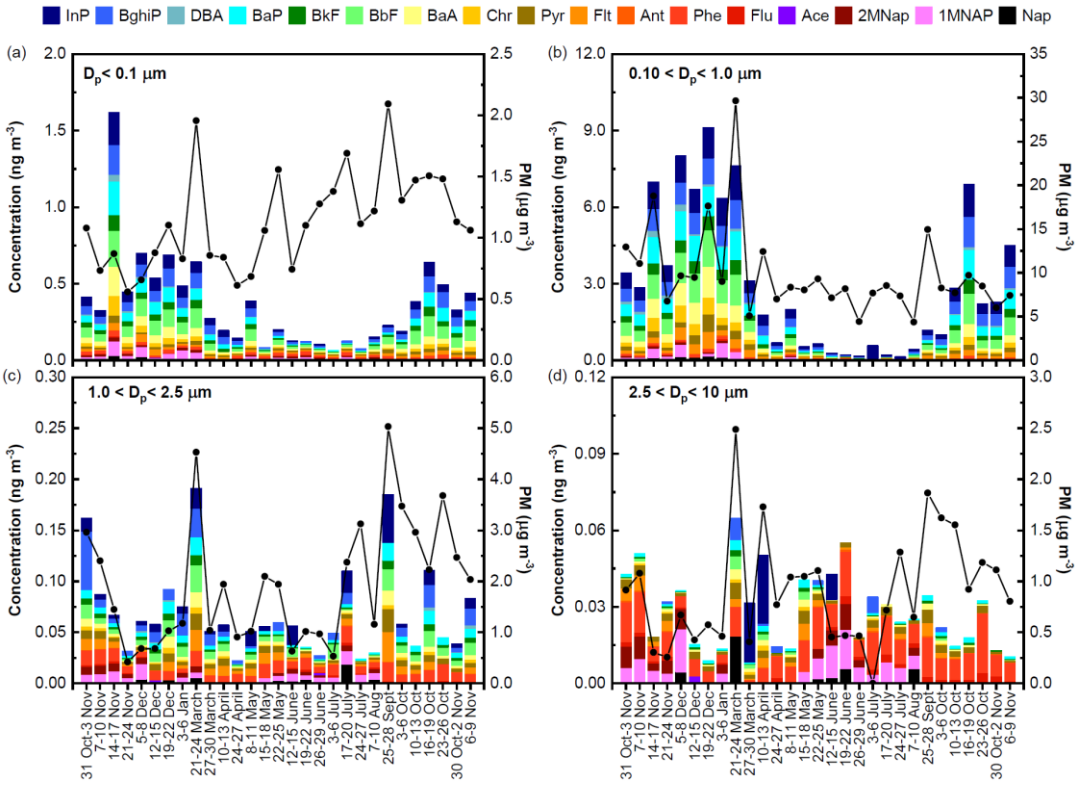

Figure II.1.6: Temporal variability of the ambient particulate matter (PM) mass concentration

(solid line) and of the PAHs identified and quantified in the four aerosol size fractions: Dp < 0.1 µm **(a)**, 0.1 < Dp < 1.0 µm **(b)**, 1.0 < Dp < 2.5 µm **(c)**, and 2.5 < Dp < 10 µm **(d)**.

Figure II.1.7 presents the size-resolved mass concentration distributions for the selected PAHs (Phe, Flt, BaP). Most of the analysed species exhibit a monomodal profile, peaking in the accumulation mode (0.1-1.0 µm), with maxima at 381 nm.

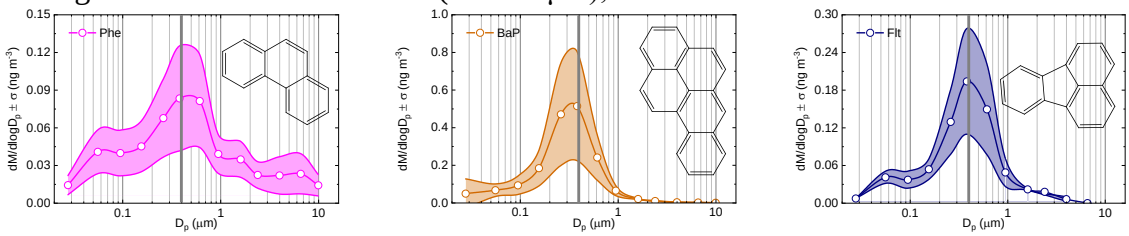

Figure II.1.7: Size-resolved mass concentration distributions of Phe **(a)**, Flt **(b)**, and BaP **(c)** in atmospheric aerosols collected from the urban area of Iasi.

Two source-apportionment approaches were applied for PAHs: PMF (positive matrix factorisation) and CWT (concentration-weighted trajectory). **Figure II.1.8** presents the CWT results for PAH sources in the PM_{10} fraction, using the mean PMF factor contributions to total PM_{10}. The 48 h air-mass back trajectories at 500 m altitude (**Figure II.1.8a**) provided the basis for the subsequent CWT analysis. The spatial distributions in **Figure II.1.8b-d** indicate hotspots, including along the Black Sea coastal region, suggesting potential PAH reservoirs in sediment-derived particles resuspended by wave action and strong winds.

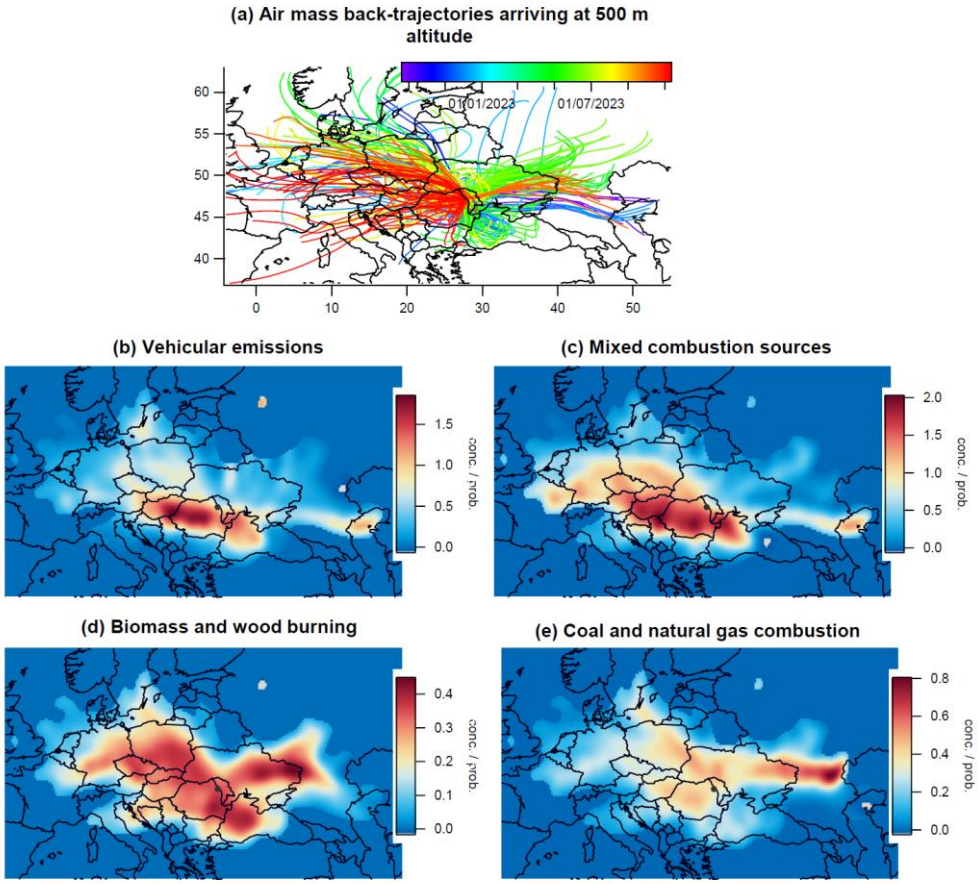

Figure II.1.8: CWT-based distribution maps obtained using 48 h air-mass back trajectories arriving at the site of interest at 500 m altitude **(a)**, and for PAH emission source regions: **(b)** traffic-related emissions; **(c)** mixed combustion sources; **(d)** biomass and wood burning; and **(e)** coal and natural gas combustion.

At the site of interest described in **Chapter II.2**, *Alternaria destruens* was identified-a species with the potential to translocate bacterial populations exhibiting different PAH uptake mechanisms (Alvarez-Barragan et al., 2023). PAHs appear to be relatively homogeneously distributed within fungal cells, likely via diffusion; a hydrophobic cell surface could promote bacterial interactions and selection in the presence of PAHs.

Chapter II.2 provides evidence for the presence of the bacterium *Priestia aryabhattai*, capable of both aerobic and anaerobic growth. Oxygen depletion during the development of *A. destruens* hyphae may generate anoxic niches that facilitate the dispersal of facultative/anaerobic bacteria through the fungal translocation network. In addition, *P. aryabhattai* could be translocated through hydrophobic zones (hydrophobic, PAH-contaminated particles) along fungal networks. These observations are ecologically relevant: aerobic and anaerobic bacteria can be dispersed-particularly translocated through hydrophobic zones-along fungal networks, thereby promoting colonisation of new niches (Alvarez-Barragan et al., 2023).

II.2 BIOAEROSOLS IN AMBIENT PARTICULATE MATTER FROM THE URBAN AREA OF IASI, NORTH-EASTERN ROMANIA. MICROBIOLOGICAL CHARACTERISATION

II.2.1 Passive sampling of bioaerosols in the urban area of Iasi

Bioaerosol samples were collected in Iasi, north-eastern Romania, at the Air Quality Monitoring Station (AMOS; latitude 47º9' N and longitude 27º35' E) of "Alexandru Ioan Cuza" University of Iasi.

Passive sampling (by gravitational settling/deposition) was carried out on 06 July 2023 and 24 April 2024. The sampling strategy on 06 July 2023 aimed to compare the microbiota at ground level (1 m), in the vicinity of Building A of "Alexandru Ioan Cuza" University of Iasi, with that specific to an altitude of 35 m above ground level at the AMOS station located on the roof of Building C (**Figure II.2.1a**). During the event on 24 April 2024, dynamic sampling was also performed simultaneously using an assembly consisting of stacked filter units (SFU) and pumps (**Figure II.2.1b**).

At the AMOS station, meteorological parameters (ambient air temperature, relative humidity (RH), total solar radiation, wind speed, and wind direction) are measured using a Hawk GSM-240 weather station (Weather Hawk, Logan, USA). Mean values of the meteorological parameters associated with the two sampling events are presented in **Table II.2.1.**

Table II.2.1: Mean values of the meteorological parameters for the passive sampling events.

Sampling event	Temperature (°C)	Humidity (%)	Solar radiation (W m^{-2})	Wind speed (m s^{-1})
2023	28,2	42,2	835	5,7
2024	19,2	49,9	381	5,8

For passive sampling, Petri dishes (Ø 100 mm) containing Luria-Bertani (LB) and Sabouraud (SAB) culture media were used. The plates were placed on tables at ~1 m height and away from obstacles to minimise cross-contamination. The standard exposure time was 1 h; to assess the effect of exposure duration, additional deployments of 2, 3, and 4 h were also performed. All components were sterilised beforehand in a microbiological safety cabinet (SafeFast Premium, vertical laminar flow), and the glassware (Petri dishes) was autoclaved (Prestige Medical, Podiaclave).

(a)

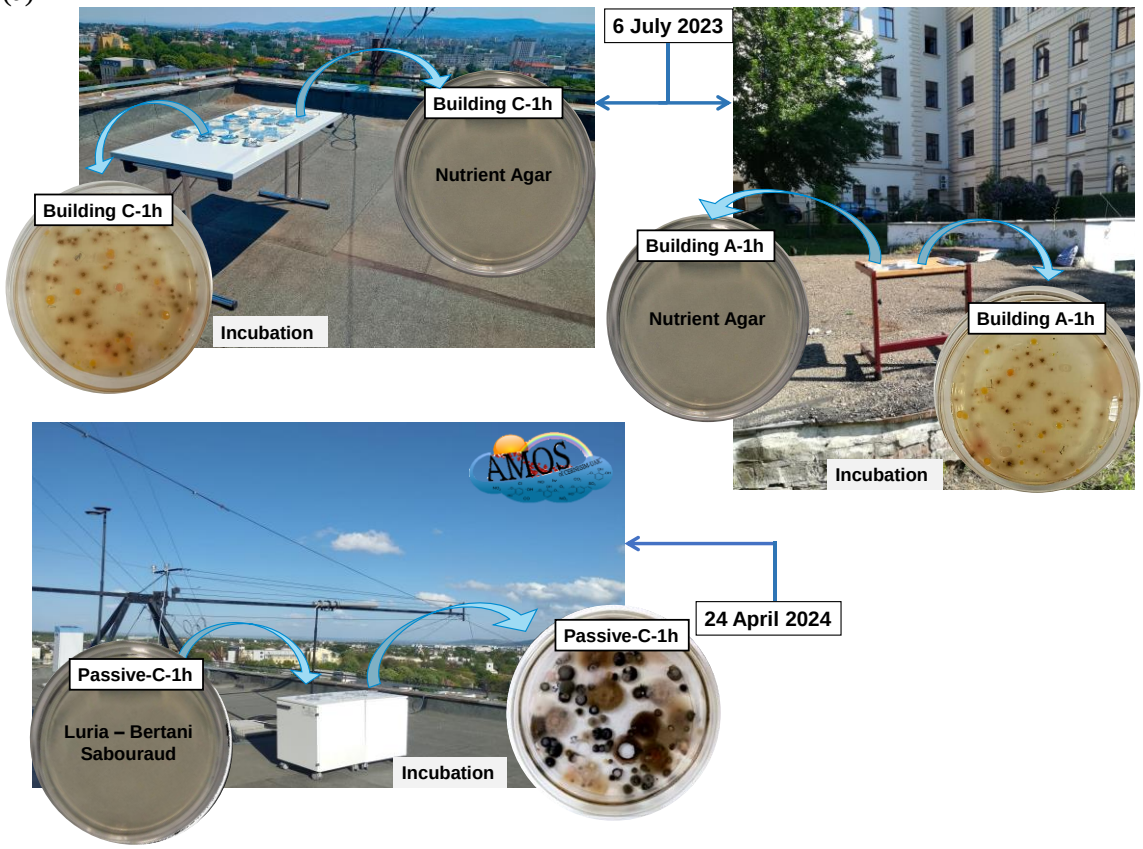

(b)

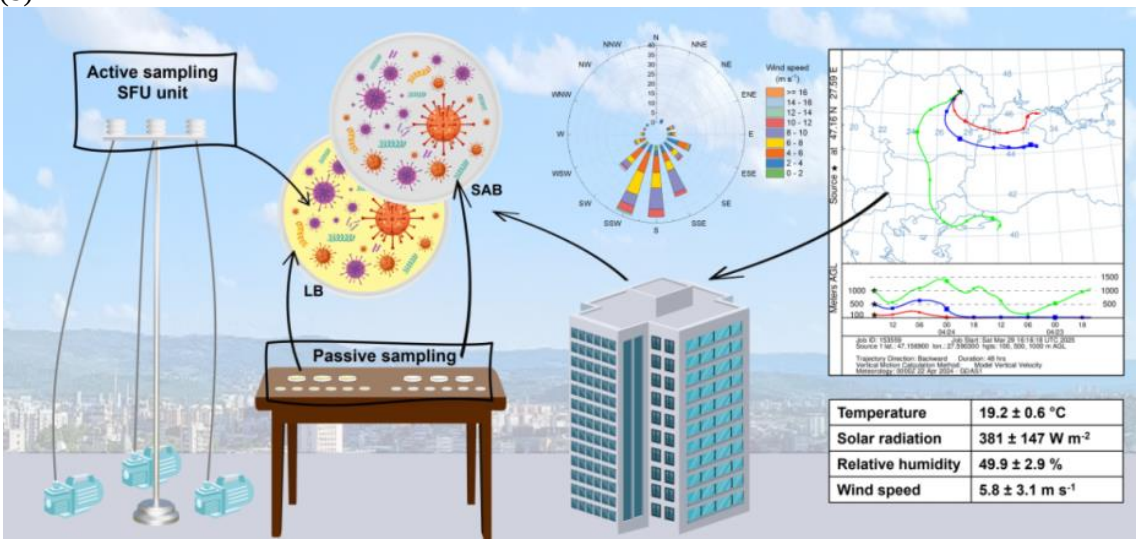

Figure II.2.1: Passive sampling strategy applied for collecting bioaerosol samples from ambient particulate matter in the urban area of Iasi during the events of 06 July 2023 and 24 April 2024 (**Figure II.2.1a**), with details of the active sampling shown in **Figure II.2.1b**.

For the (active) SFU-based sampling, the SFU components were cleaned with 70% ethanol and subsequently UV-sterilised. Each SFU was connected to a pump and a flow meter, with a sampled air volume of 1.78 m^3 h^{-1}. For both events, field blanks/control samples were included to assess potential cross-contamination. Air-mass back trajectories arriving at the sampling location (**Figure II.2.2**) were generated using HYSPLIT 4 (ARL/NOAA) via the READY platform (Stein et al., 2015; Rolph et al., 2017) for a 48 h period. In 2023, air masses arrived predominantly from the NE and SE (Ukraine and the Republic of Moldova) (**Figure II.2.2a**). In 2024, trajectories computed at 100, 500, and

1000 m indicate a predominantly south-easterly origin (the Black Sea region) (**Figure II.2.2b**).

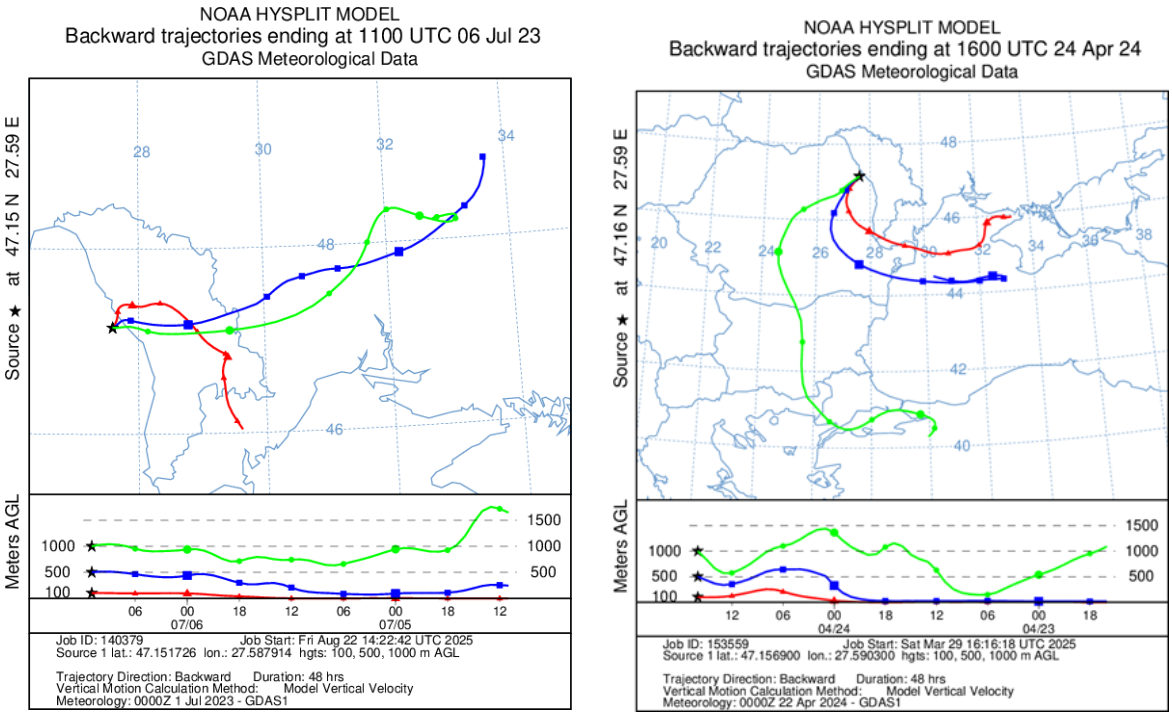

(a) **(b)**

Figure II.2.2: Air-mass back trajectories arriving at the sampling sites for the event on 06 July 2023 **(a)** and 24 April 2024 **(b)**.

II.2.2 Preparation of bioaerosol samples

Samples collected by passive sampling were incubated directly upon arrival in the laboratory. For samples collected under dynamic sampling conditions, two inoculation approaches were used, schematically shown in **Figure II.2.3.**

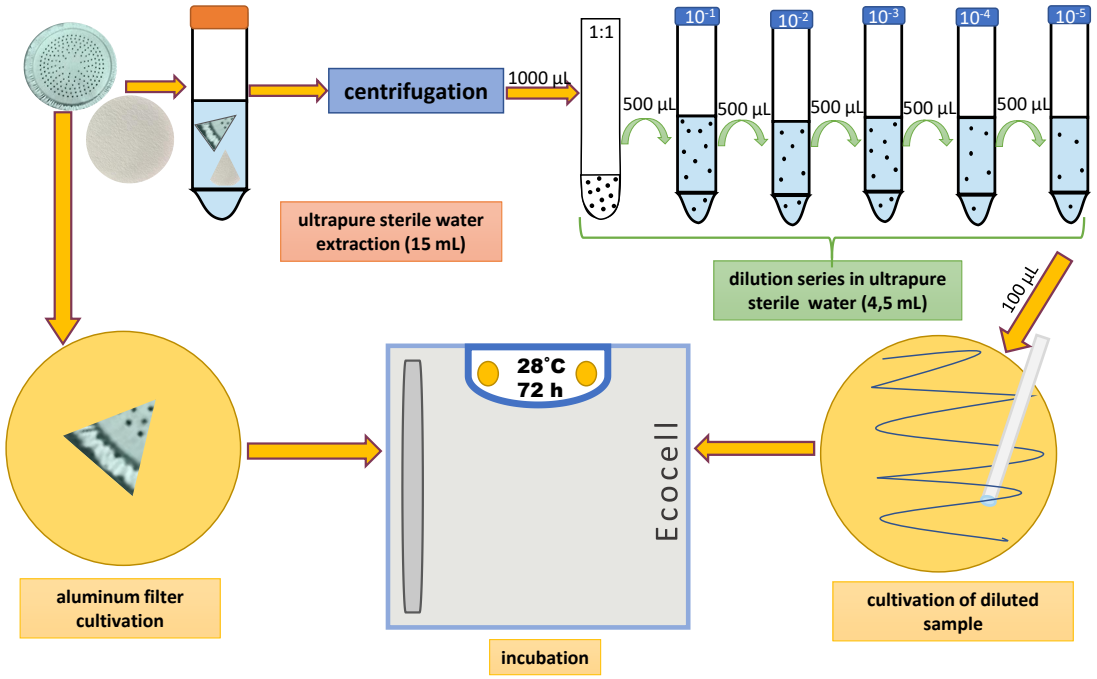

Figure II.2.3: Steps followed for inoculating bioaerosol samples collected under dynamic sampling conditions.

For the first approach, filters loaded with bioaerosol samples (or blank filters) were placed directly onto Petri dishes previously prepared with nutrient-rich growth media (LB or SAB). In the second approach, the collected bioaerosols were extracted, and the resulting extracts were subsequently used for inoculation onto Petri dishes pre-prepared with the appropriate culture media (LB or SAB).

For extraction, exposed filters and blank samples were transferred into sterile Eppendorf tubes pre-filled with nutrient-rich LB or SAB medium; extraction was performed using a vortex system at 2000 rpm for 1 min. Aliquots of 100 µL of the extracts were pipetted and evenly spread over the surface of the pre-prepared LB or SAB Petri dishes using an inoculation loop. Quartz blank control filters were subjected to a similar preparation procedure. The extracts were serially diluted from 10^{-3} up to 10^{-5}. Petri dishes obtained from both passive and active sampling, including blanks, were incubated at 28 ºC in a natural-convection incubator (Ecocell, Germany), with continuous monitoring during the first 24 h and subsequently at 24 h intervals over an extended period. After incubation, microbial cultures were stored at 2-4 ºC in an Infrico Medcare LTUF258 laboratory refrigerator.

II.2.3 Microbiological characterisation of bioaerosols in ambient particulate matter from the urban area of Iasi

Figures II.2.4 and II.2.5 show details of Petri dishes at different incubation stages for the samples collected on 06 July 2023 and 24 April 2024. Visible microorganisms were subsequently isolated and purified to maintain viable cultures and to enable genus/species identification, using sterile inoculation loops (1 µL) onto Petri dishes containing culture media (LB or SAB). In **Figure II.2.4**, red arrows indicate bacteria (B) and blue arrows indicate fungi (F); in Figure II.2.5, red indicates bacteria (B), blue indicates fungal colonies (F), and green indicates yeasts (Y).

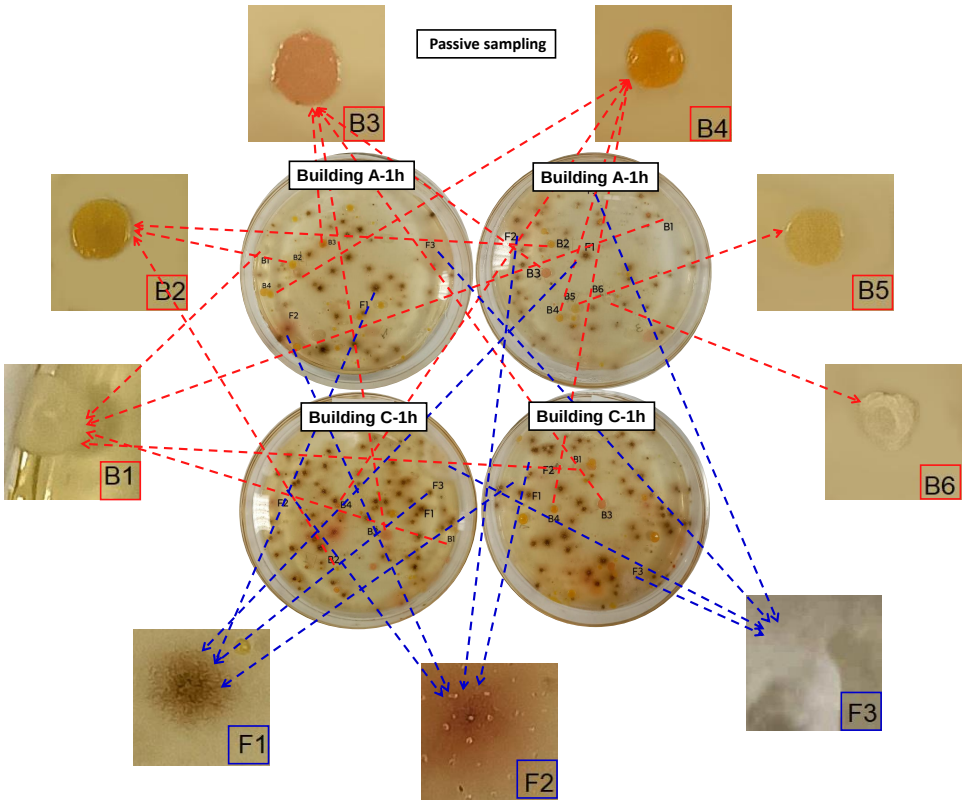

Figure II.2.4: Appearance of the Petri dishes for samples collected on 06 July 2023 by passive sampling, at ~1 m above ground level (Building A) and at 35 m above ground level (Building C), after incubation at 28 ºC for specific time periods.

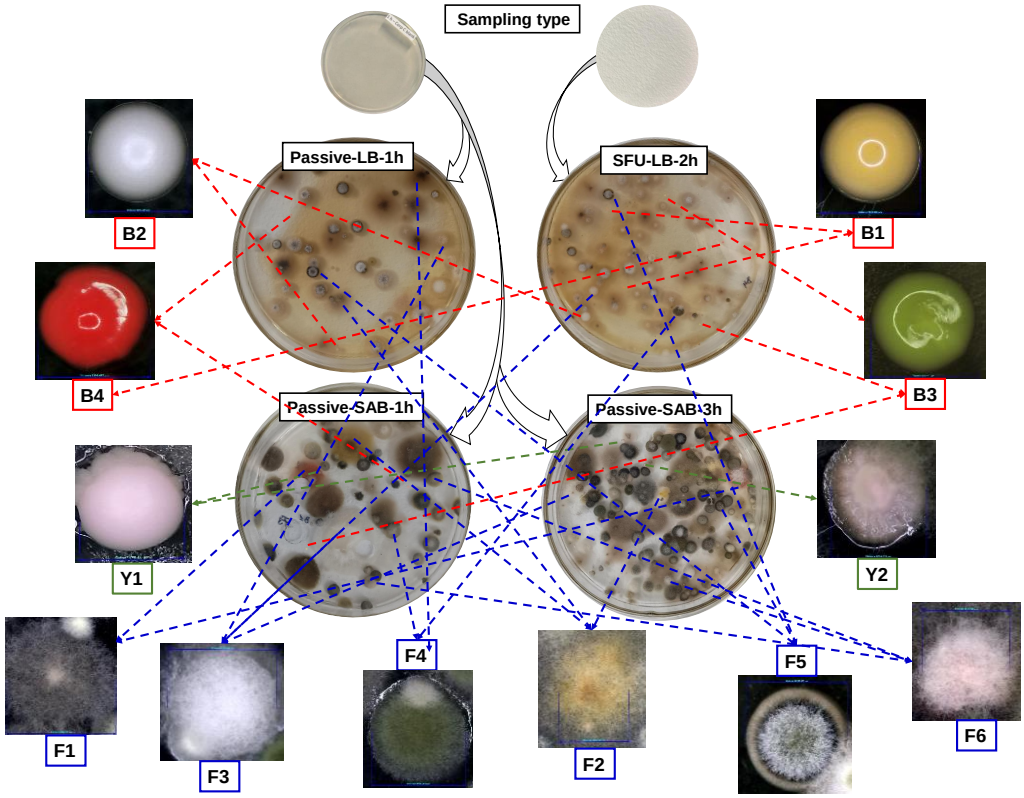

Figure II.2.5: Appearance of the Petri dishes for samples collected on 23 April 2024 by passive or dynamic sampling, at 35 m above ground level (Building C), after incubation at 28 ºC for specific time periods.

Microbial colonies isolated and purified from the particulate matter samples were examined at RECENT AIR (Romania), primarily using conventional optical microscopy. Genus- and species-level identification was performed as an outsourced service by Eurofins BIOMI Ltd. (Gödöllő, Hungary).

For the 24 April 2024 sampling event, within the first 24 h the microbial colonies B1, B2 and the fungal colonies F1, F3 appeared, with pronounced proliferation of bacterium B2 after 12 h. B3 and B4 developed after 48 h; the yeasts Y1, Y2 and the fungal colony F2 after 72 h; and F4 and F5 after 10 days. Colony F6 appeared within 24 h but subsequently died during storage at 2-4 ºC. The Y1 and Y2 colonies, pink and with an apparently bacterial morphology, were confirmed as yeasts only after microscopic examination or sequencing.

II.2.3.1 Morpho-structural characterisation of bioaerosols

For the morphological characterisation of bioaerosols from ambient particles collected in Iasi, after sample preparation the Stemi 508 KMAT stereomicroscope (Carl Zeiss GmbH, Germany) was used, enabling colony-level observation and classification of bacteria, fungi, and yeasts grown on culture media.

Table II.2.2 presents morphological details for selected bacterial and fungal colonies from plates corresponding to the 06 July 2023 event, while **Table II.2.3** provides similar information for the 24 April 2024 event. In addition, Gram staining was performed to obtain more specific information regarding the types of bacteria present in the samples. The experimental steps of the Gram-staining procedure are shown in **Figure II.2.6**.

Gram staining was carried out using crystal violet and fuchsin to classify bacteria as Gram-positive (purple cells) or Gram-negative (pink cells).

Table II.2.2: Selected morphological characteristics of bacterial and fungal colonies isolated from particulate matter samples collected during the 06 July 2023 event.

B1 (Building A, ~ 1 m)	**B2** (Building C, ~ 35 m)	**B3** (Building A, ~ 1 m)
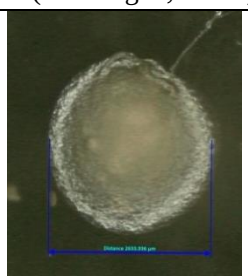		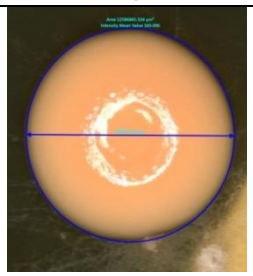
White bacterial colony, smooth, glossy surface and regular edge,, Ø = 2,63 mm	Yellow bacterial colony, smooth, glossy surface and regular edge, Ø = 3,65 mm	Pink bacterial colony, smooth, glossy surface and regular edge, Ø = 4,00 mm
B4 (Building A, ~ 1 m)	**B5** (Building A, ~ 1 m)	**B6** (Building A, ~ 1 m)
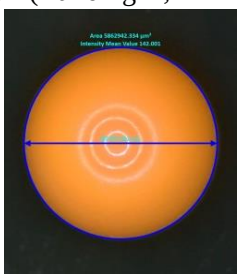	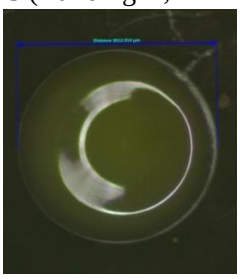	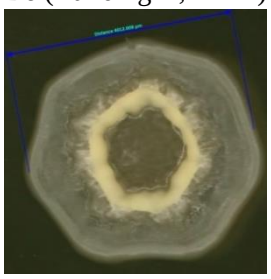
Orange bacterial colony, smooth, glossy surface and regular edge, Ø = 2,73 mm	Yellowish bacterial colony, smooth, glossy surface and regular edge, Ø = 3,61 mm	White bacterial colony, crater-shaped and irregular edge,, Ø = 4,01 mm
F1 (Building C, ~ 35 m)	**F2** (Building A, ~ 1 m)	**F3** (Building A, ~ 1 m)
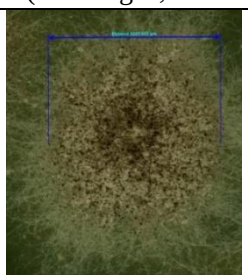	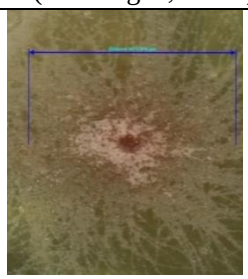	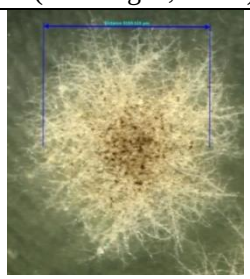
Brown fungal colony, Ø = 3,24 mm	Pink fungal colony, Ø = 3,67 mm	White fungal colony, Ø = 3,13 mm

Table II.2.3: Morphological details of bacterial, fungal, and yeast-like colonies isolated from particulate matter collected during the 24 April 2025 event (Building C, ~35 m above ground level).

Bacteria (B)			
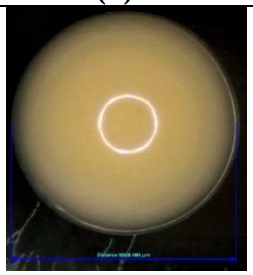		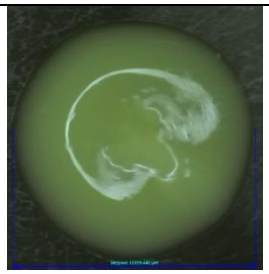	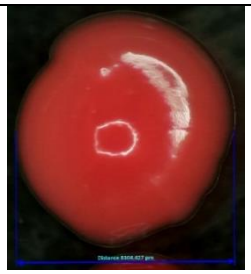
B_1 – Orange bacterial colony, smooth, glossy surface and regular edge, Ø = 9.04 mm	**B_2** – White bacterial colony, smooth, glossy surface and regular edge, Ø = 9.20 mm	**B_3** – Yellow bacterial colony, smooth, glossy surface and regular edge, Ø = 11.35 mm	**B_4** – Red bacterial colony, smooth, glossy surface and regular edge, Ø = 8.30 mm

Fungi (F) and Yeast (Y)			
 **F_1** – Light pink fungal colony, Ø = 11.40 mm	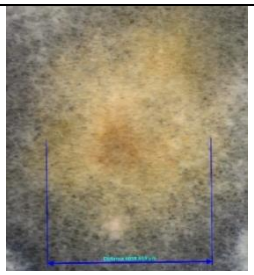 **F_2** – Brown fungal colony, Ø = 6.66 mm	 **F_3** – White fungal colony, Ø = 11.22 mm	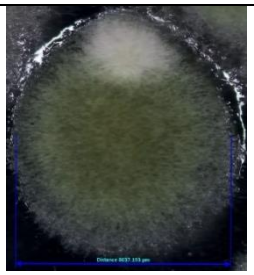 **F_4** – Green fungal colony, Ø = 8.63 mm
 **F_5** – Green fungal colony, Ø = 8.64 mm	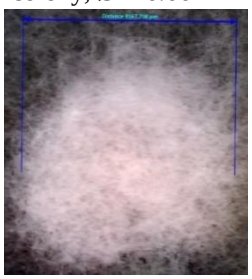 **F_6** – Dark pink fungal colony, Ø = 8.17 mm	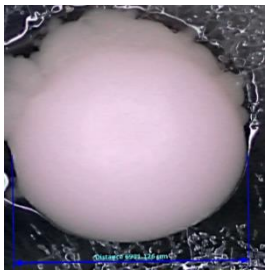 **Y_1** – Pale pink yeast colony, smooth, glossy surface and regular edge, Ø = 6.90 mm.	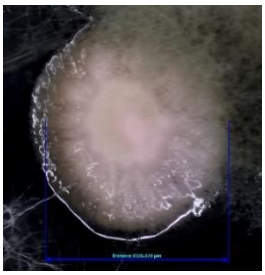 **Y_2** – Dark pink yeast colony, rough and glossy surface and regular edge, Ø = 8.03 mm.

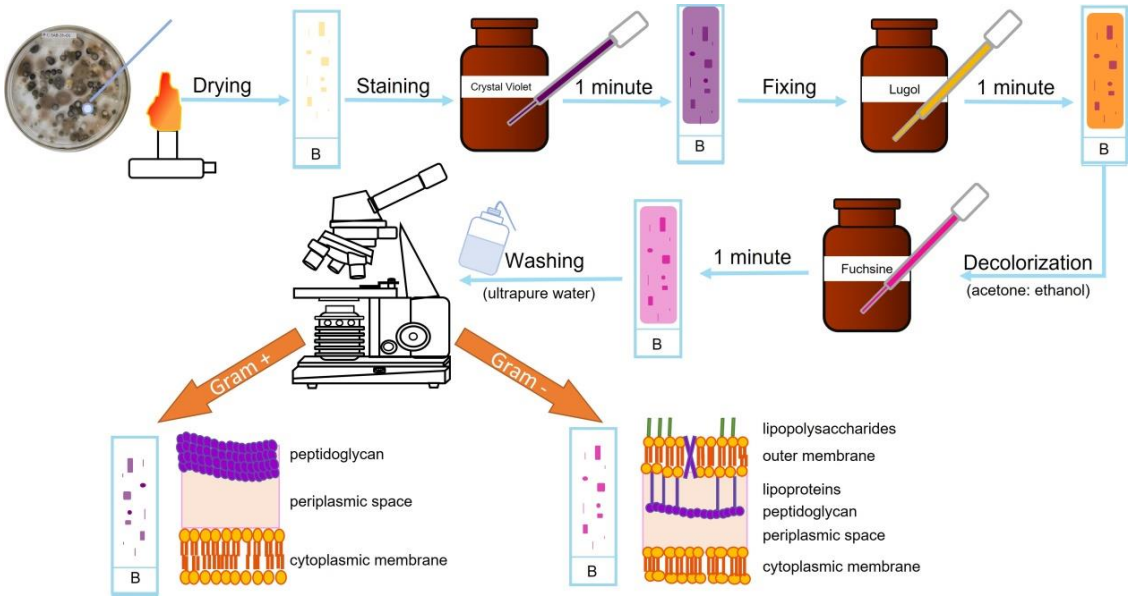

Figure II.2.6: Experimental steps followed in the Gram-staining procedure.

The results obtained from Gram staining and microscopic examination of the smears are presented in **Table II.2.4** for the 06 July 2023 sampling event and in **Table II.2.5** for the 24 April 2024 event.

Microorganisms D1 and D2 in **Table II.2.5** were initially presumed to be yeasts based on the blastospores revealed by Gram staining. In the samples from the analysed event, yeast-like fungal colonies were observed, in which asexual conidia formed by budding of yeast-like cells (blastospores) were identified.

Table II.2.4: Anatomical-structural details obtained by Gram staining for microorganisms isolated from ambient particulate matter associated with the 06 July 2023 event.

Bacteria (B)	
Building A, ~ 1 m above ground level	**Building C, ~ 35 m above ground level**
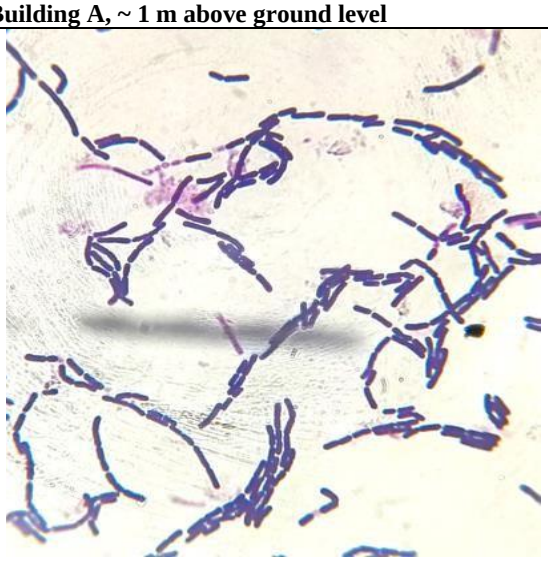	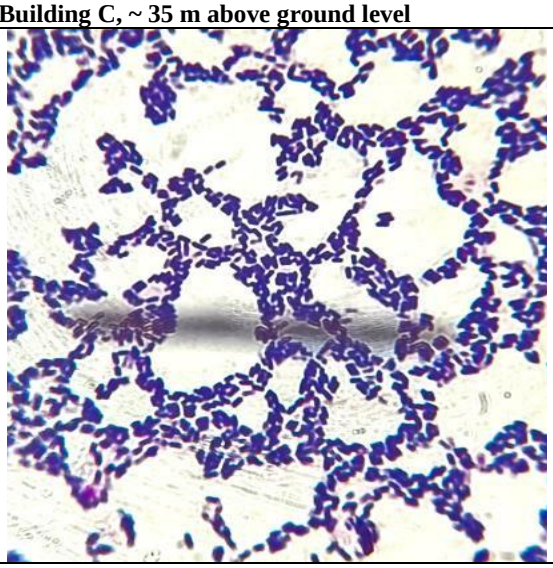
B_{11} – Gram+ bacteria, bacilli – mono- and diplobacilli (1000×), white bacteria	**B_{12}** – Gram+ bacteria, bacilli – mono- and diplobacilli (1000×), translucent bacteria
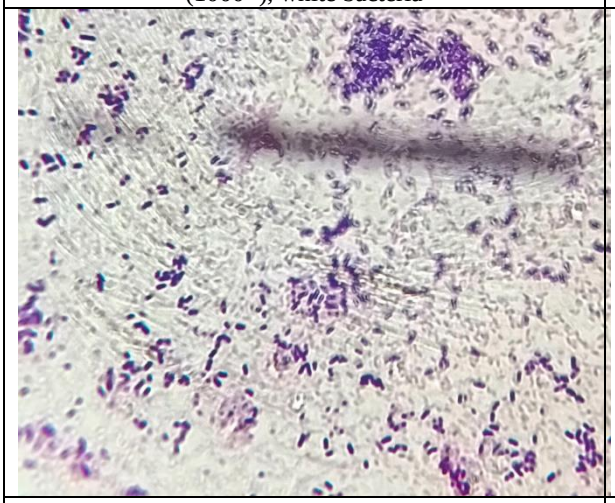	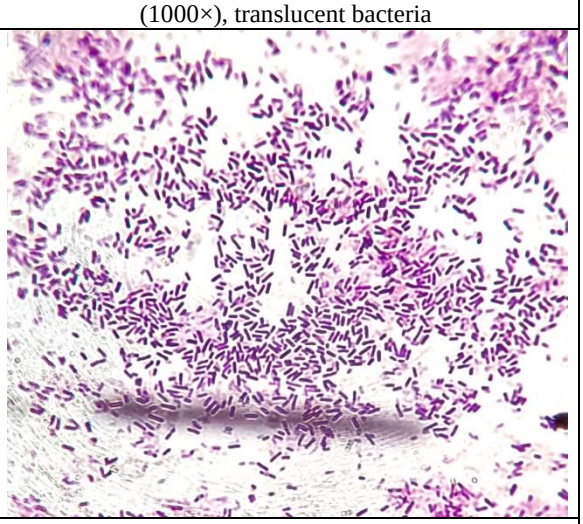
B_{13} – Gram+ bacteria, coccobacilli (1000×), whitish bacteria	**B_{14}** – Gram+ bacteria, , bacilli – mono- and diplobacilli (1000×), whitish bacteria
	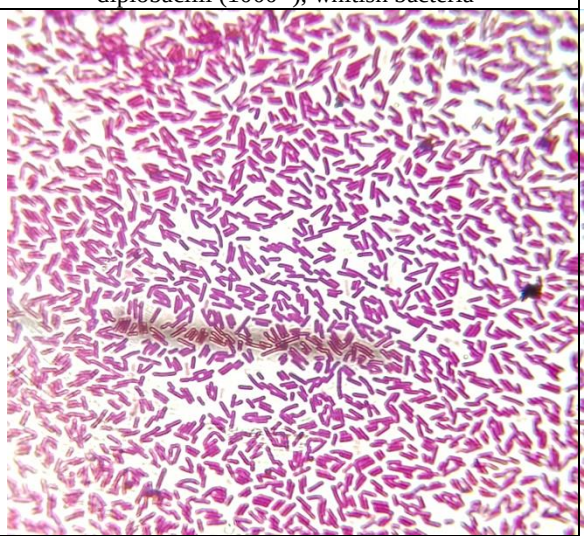
B_{33} – Gram- bacteria, bacili – mono-, diplo- and streptobacilli (1000×), salmon orange bacteria	**B_{34}** – Gram- bacteria, bacilli – mono- and diplobacilli (1000×), salmon orange bacteria

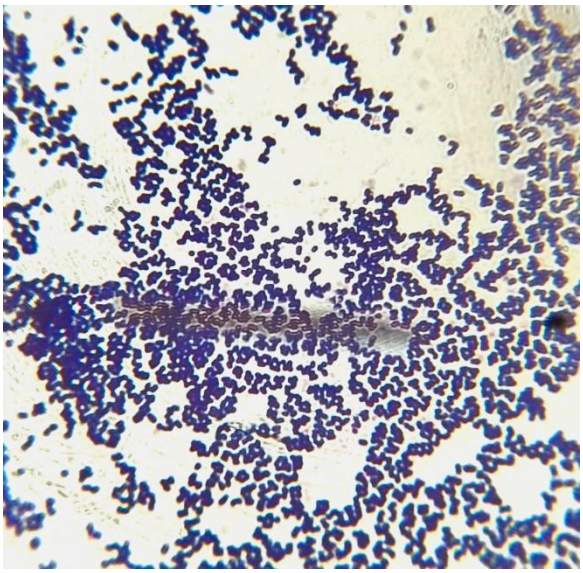	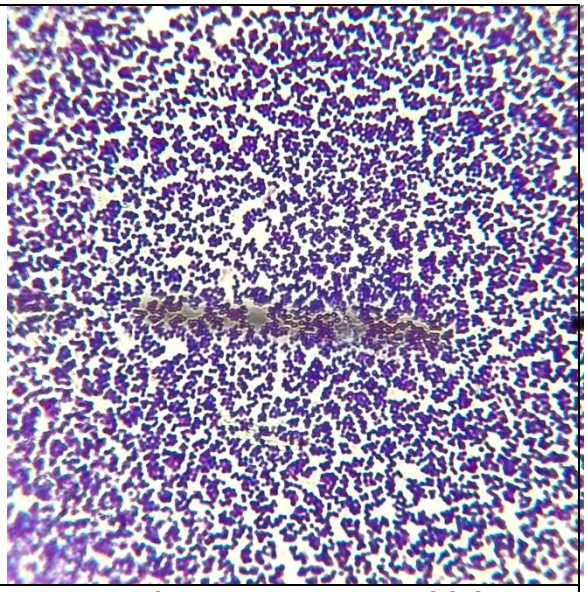
B_{41} – Gram+ bacteria, cocci – mono- and diplococci and tetrade (1000×), bright orange bacteria	**B_{42}** – Gram+ bacteria, cocci – mono- and diplococci and tetrade (1000×), bright orange bacteria
Fungi (F)	
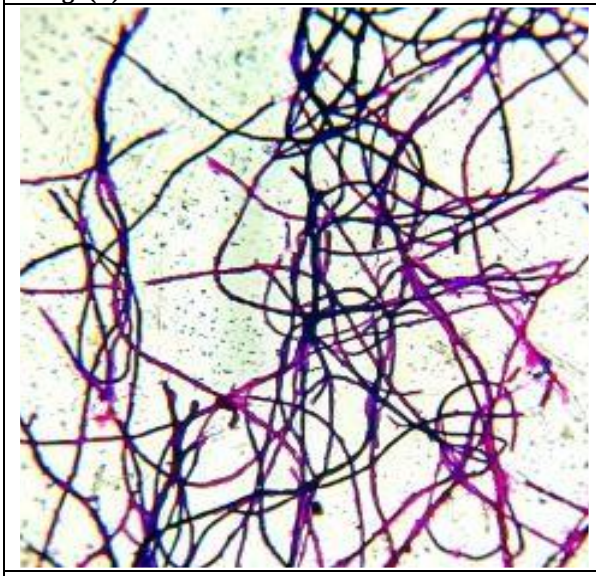	
F_{11} – Mycelia (400×)	**F_{12}** – Mycelia (400×) and spores (1000×)
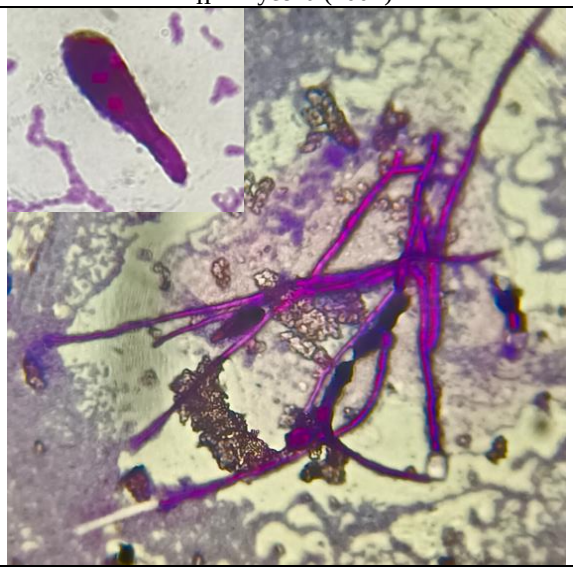	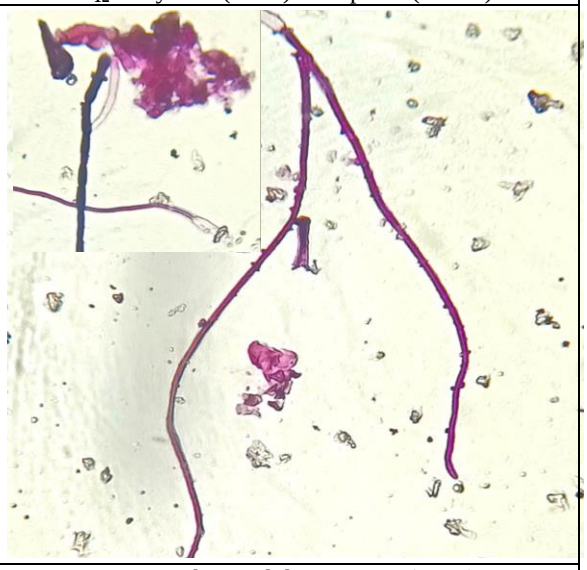
F_{13} – Hyphae and dictiospores (400×)	**F_{14}** – Hyphae and dictiospores (400×)

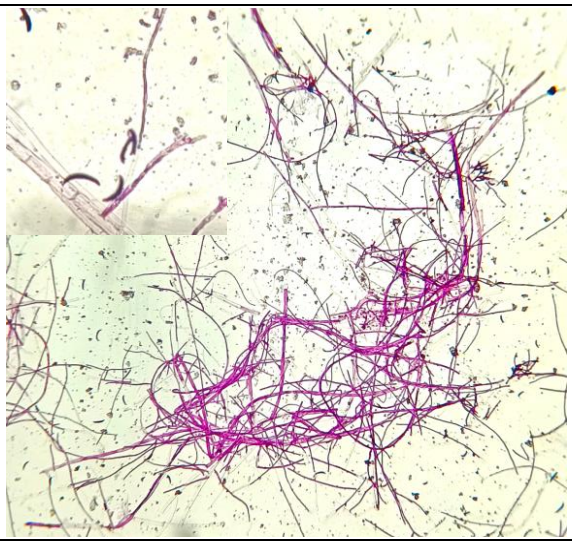	
F_{31} - Mycelia (100×) and microconidia (400×)	**F_{32}** - Hife (100×) and monophialides (400×)

Tabelul II.2.5: Anatomical-structural details obtained by Gram staining for microorganisms isolated from ambient particulate matter associated with the 24 April 2024 (Body C, 35 m above ground level) event.

Bacteria (B)	
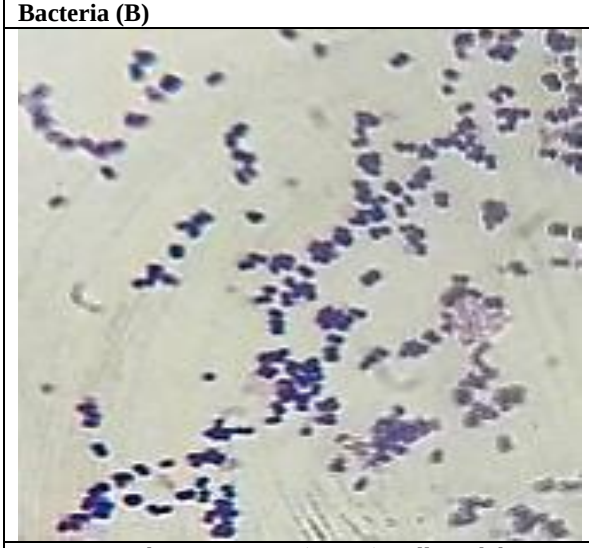	
B_1 – Gram+ bacteria, cocci (1000×), yellowish bacteria	**B_2** – Gram+ bacteria, bacilli (1000×), white bacteria
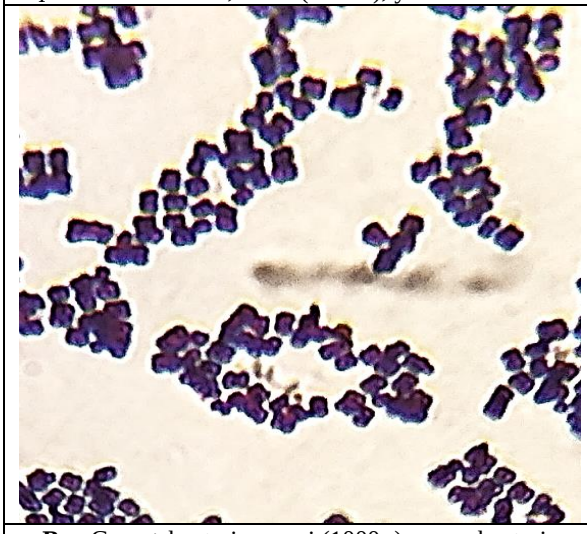	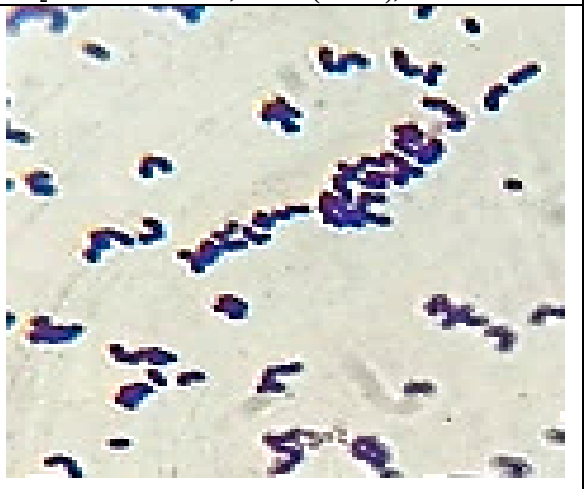
B_3 – Gram+ bacteria, cocci (1000×), green bacteria	**B_4** – Gram+ bacteria, coccobacilli (1000×), red bacteria

Fungi (F)	
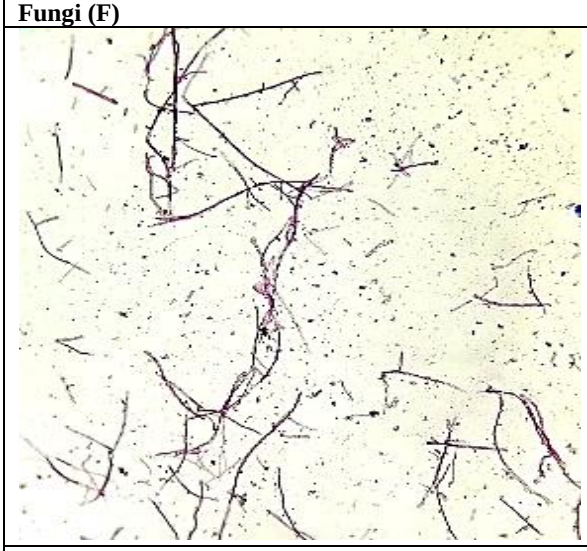	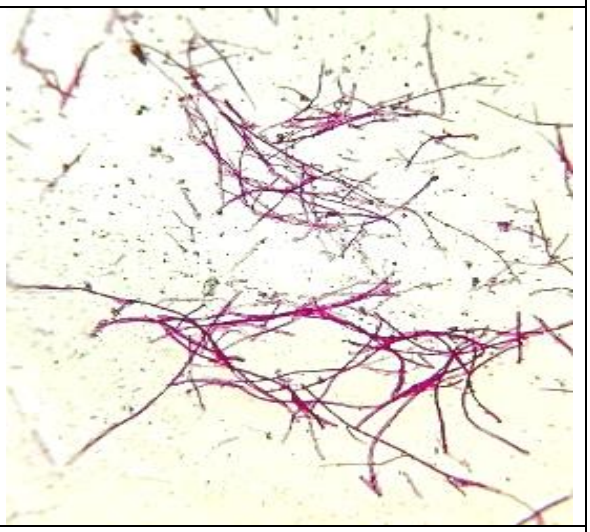
F_1 – Mycelia (100×)	**F_1** – Mycelia (400×)
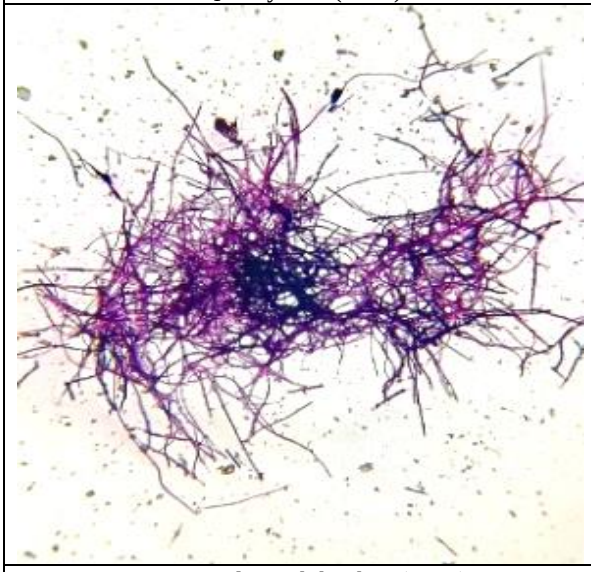	
F_2 – Mycelia with hyphae (100×)	**F_2** – Mycelia with conidiophores (400×)
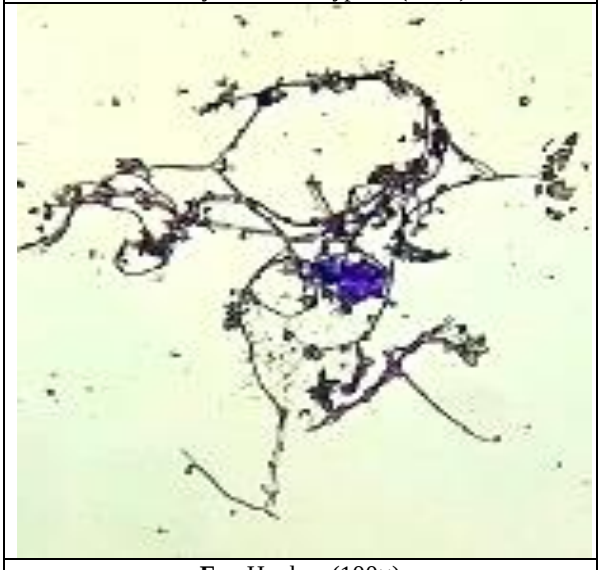	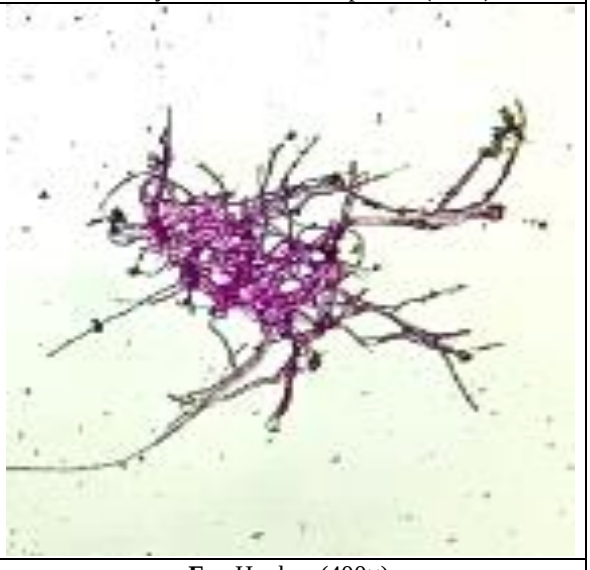
F_3 – Hyphae (100×)	**F_3** – Hyphae (400×)

F_4 – Mycelia with hyphae (100×)

F_4 – Mycelia with conidiophores (400×)

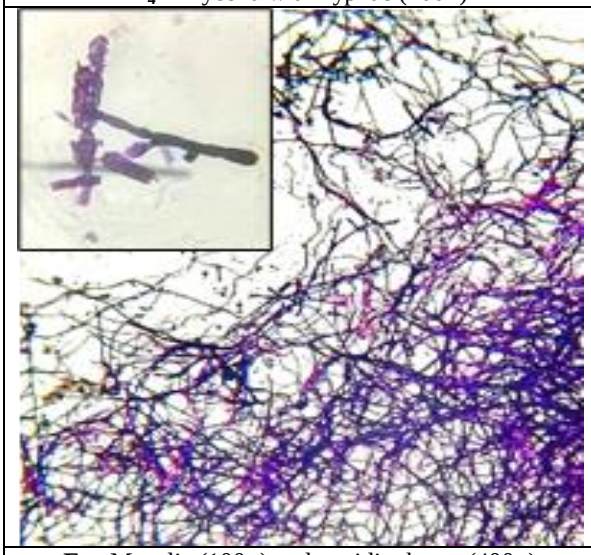

F_5 – Mycelia (100×) and conidiophores (400×)

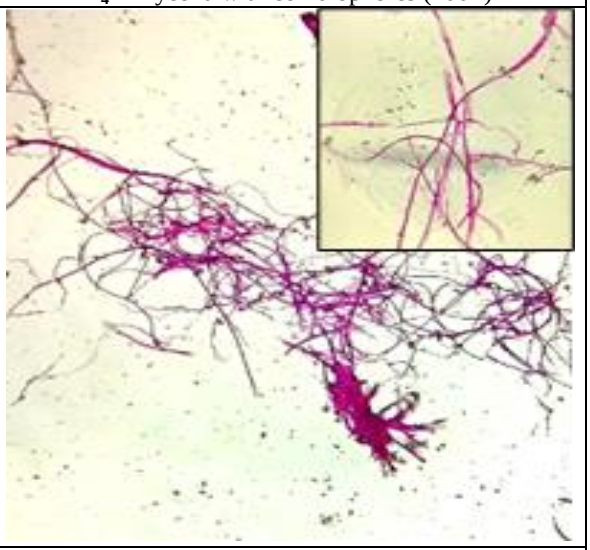

F_6 – Mycelia (100×) and hyphae (400×)

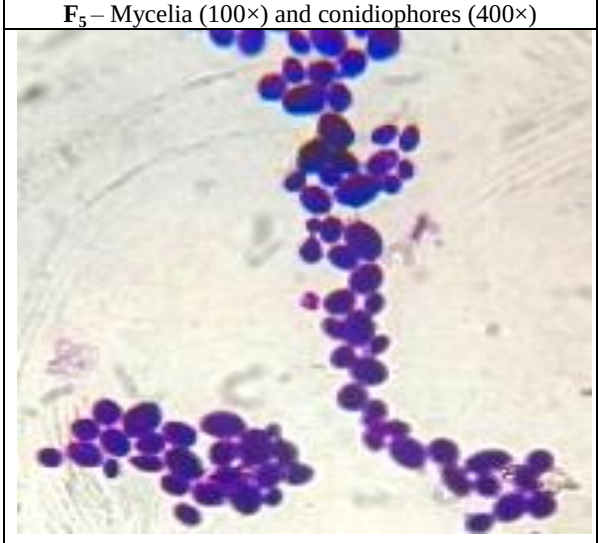

Y_1 – Yeast, blastospores (1000×)

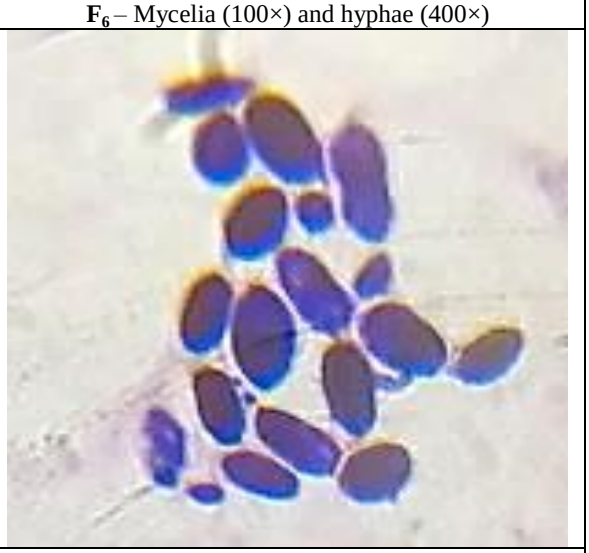

Y_2 – Yeast, blastospores (1000×)

II.2.3.2 Identification of microorganisms isolated from bioaerosol samples in the urban atmosphere of Iasi

The results on genus- and species-level identification of microorganisms isolated from bioaerosols associated with urban particulate matter in Iasi (24 April 2024 event) are presented in **Table II.2.6**, although the analyses were not carried out in laboratories in Romania.

Identification (to genus/species level) was performed as an outsourced service by Eurofins BIOMI Ltd. (Gödöllő, Hungary) and was essential for subsequent investigations. For bacteria, the 16S rRNA gene region was sequenced, whereas for fungi and yeasts the ITS1–2 region was analysed, using standard PCR and qPCR methods.

Table II.2.6: Microbial species identified or detected in microorganisms isolated from particulate matter collected in the urban area of Iasi.

Code	Microbial system	Microbial genus	Hit microbial species	Sample code		Experimental detail
				Analisys	Discussions	
B_1	Bacteria	*Planococcus*	*Planococcus wigleyi*	B_1-$Pla_{i=1-3}$	$B_{Pla.\ wig.}$	
B_2		*Priestia*	*Priestia aryabhattai*	B_2-$Pri_{i=1-2}$	$B_{Pri.\ ary.}$	
B_3		*Agrococcus*	*Agrococcus citreus*	B_3-$Agr_{i=1-3}$	$B_{Agr.\ cit.}$	
B_4		*Arthrobacter*	*Arthrobacter sp.*	B_4-Arh	$B_{Arh.\ sp.}$	
F_1	Fungi	*Fusarium*	*Fusarium*	F_1-$Fus_{i=1-3}$	$F_{Fus.}$	
F_2		*Alternaria*	*Alternaria destruens*	F_2-$Alt_{i=1-2}$	$F_{Alt.\ des.}$	
F_3		*Alternaria*	*Alternaria sp.*	F_3-$Alt_{i=1-2}$	$F_{Alt.\ sp.}$	
F_4		*Cladosporium*	*Cladosporium sp.*	F_4-$Cla_{i=1-2}$	$F_{Cla.\ sp.\ 1}$	
F_5				F_5-$Cla_{i=1-2}$	$F_{Cla.\ sp.\ 2}$	
F_6		-	-	-	-	
Y_1	Yeast	*Aureobasidium*	*Aureobasidium sp.*	D_1-$Aur_{i=1-3}$	$D_{Aur.\ sp.\ 1}$	
Y_2				D_2-$Aur_{i=1-3}$	$D_{Aur.\ sp.\ 2}$	

Planococcus wigleyi (B1) is frequently isolated from chicken faeces (Pallen, 2024). *Priestia aryabhattai* (B2), a member of the genus *Priestia* and formerly classified within *Bacillus* (Gupta et al., 2020), has been reported from soil, wastewater, and electronic waste; it shows potential for the biodegradation of e-polymers/pesticides (Hanano et al., 2025; Chakraborty et al., 2023) and for metal bioremediation (Nithyashree and Subramanian, 2025). Plastic degradation may generate VOCs and other secondary by-products (Chakraborty et al., 2023). *Agrococcus citreus* (B3) is widely distributed in terrestrial and aquatic ecosystems and has been associated with plants, fungi, animals, and

clinical specimens (Evtushenko and Takeuchi, 2006). *Arthrobacter sp*. (B4) has been reported from desert soils (Liu et al., 2018; Guo et al., 2019). According to Eurofins BIOMI Ltd., the *Fusarium* isolate (F1) from the urban particulate matter in Iasi appears to represent a novel candidate within the genus *Fusarium*. *Alternaria destruens* (F2) was isolated from contaminated marine sediments and can grow in the presence of PAHs or translocate bacteria in hydrophobic environments (Alvarez-Barragan et al., 2023). Seasonal variability of 17 PAHs in urban aerosols from Iasi has been reported (Amarandei et al., 2024), and the detection of *A. destruens* suggests a potential role in particle chemistry. *Alternaria spp*. (F3) originates primarily from cereal crops/pastures, and the *Alternaria* allergen is abundant in air, mainly from spore and hyphal fragments (Alberto et al., 2024; Apangu et al., 2023). *Cladosporium spp*. (F4, F5) are common on living and dead plant material and have a high allergenic potential (Sindt et al., 2016). *Aureobasidium spp.* (Y1, Y2) occur predominantly in soils and on plants.

II.3 MOLECULAR AND ELEMENTAL CHARACTERISATION OF ATMOSPHERIC BIOAEROSOLS FROM THE URBAN AREA OF IASI

II.3.1 Molecular-level analysis of selected bioaerosols in ambient air from the urban area of Iasi using MALDI–Orbitrap MS for the identification of bacterial peptide markers

For microorganisms isolated from particulate matter-associated airborne bioaerosols sampled at the AMOS station on 06 July 2023, molecular investigations were performed using an Orbitrap Exploris 240 (Thermo Scientific, USA) coupled to a MALDI source (MassTech, USA), located in the RECENT AIR laboratories of "Alexandru Ioan Cuza" University of Iasi.

II.3.1.1 Bioaerosol samples

Samples analysed by MALDI–Orbitrap MS originated from passive sampling on Luria-Bertani (LB) medium. For the 06 July 2023 event, air masses arriving at the site at 07:00 UTC had a south-easterly origin (Black Sea region), whereas at 11:00 UTC they originated predominantly from the north-eastern transect; at 100 m altitude, the air mass was mainly local and strongly influenced by a thermal inversion (**Figure II.2.2b**). Sampling locations were Building A (~1 m above ground level) and Building C/AMOS (~35 m), and the sampling and preparation procedures (direct incubation, extraction, inoculation, growth, etc.) are described in **Chapters II.2.**1 and **II.2.2**.

II.3.1.2 Optimal operating conditions for MALDI–Orbitrap MS in bioaerosol investigations

Selected bacterial and fungal colonies were analysed using the Orbitrap Exploris 240 (Thermo Scientific) coupled to a MALDI source (MassTech) at RECENT AIR, "Alexandru Ioan Cuza" University of Iasi. The MALDI–Orbitrap MS protocol comprised: transfer of biomass from the culture medium into an Eppendorf tube containing 10 µL of 70% formic acid, vortexing for 3 min, addition of 10 µL acetonitrile, vortexing for 3 min, followed by spotting 0.5 µL of the supernatant onto the MALDI target plate and application of the CHCA matrix (Freiwald and Sauer, 2009).

II.3.1.3 Mass spectra of bacteria and fungi isolated from ambient bioaerosols

Contributions from the ionisation matrix and blank samples (artefacts arising from operation under sterile conditions) were subtracted from the mass spectra of the bacterial/fungal samples of interest. Spectra were acquired over the m/z 400–6000 range.

Figure II.3.1 shows: (a) the CHCA matrix spectrum; (b) the blank sample spectrum; (c) the spectrum of a bacterial isolate from ambient particulate matter-associated bioaerosols; (d) the same bacterial spectrum after subtraction of matrix and blank signals; and (e) the spectrum in (d) restricted to m/z 400–1500. For the bacterial sample coded B_{11}, the spectrum shown in **Figure II.3.1e** was evaluated, assigning compounds or compound classes using the ECMDB, MiMeDB, and LIPID MAPS databases. MS/MS spectra were also generated for selected molecular ions. The MS/MS spectra are shown in **Figure II.3.2** for the ten most intense signals in the full mass spectrum acquired over m/z 400–6000.

.

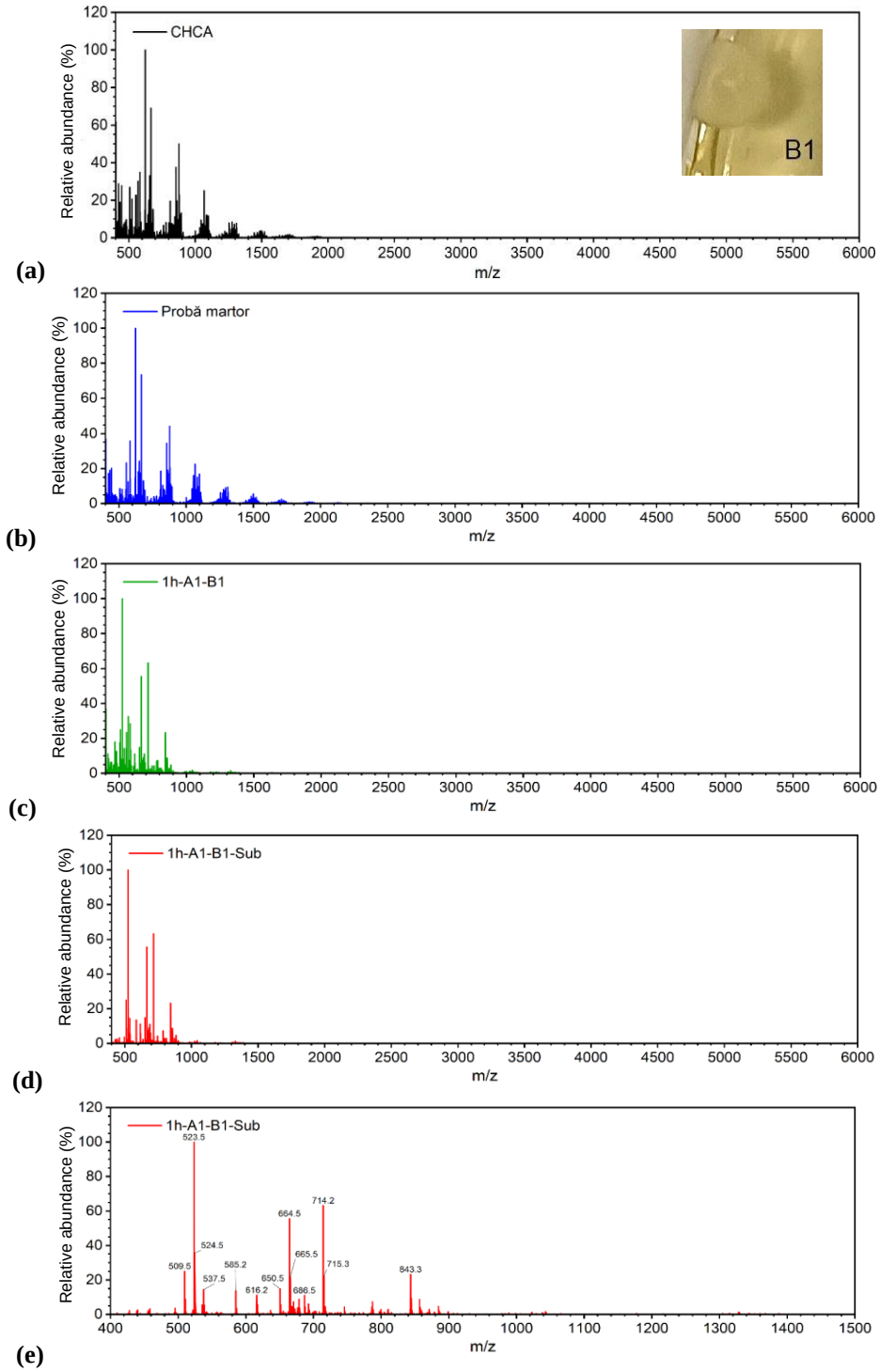

Figure II.3.1: Mass spectra acquired over the m/z 400–6000 range for α-cyano-4-hydroxycinnamic acid (CHCA) used as the ionisation matrix **(a)**, the blank sample **(b)**, the bacterial sample B_{11} **(c)**,

the bacterial spectrum after subtraction of the matrix and blank signals **(d)**, and the m/z 400–1500 mass spectrum of the bacterial sample after subtraction **(e)**.

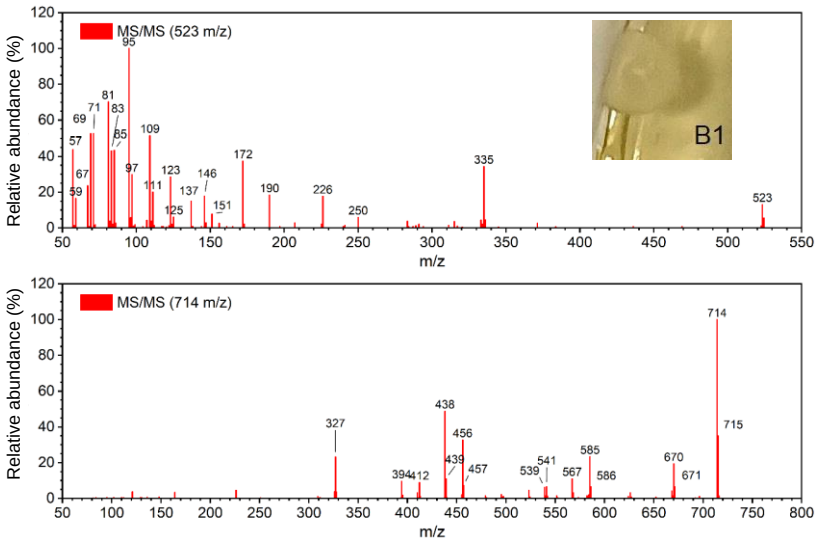

Figure II.3.2: MS/MS mass spectra for two signals from the full mass spectrum acquired over the m/z 400–6000 range for the bacterial colony B_{11}.

The MS/MS spectra highlighted characteristic signals within the m/z 50–850 range, some of which are consistent with the profiles of *Bacillus cereus* and *Bacillus thuringiensis* strains. An ion at m/z 714.2485 may correspond to a biomarker reported for the identification of *B. cereus* and its discrimination from *B. thuringiensis* (the latter being associated with a characteristic signal at m/z 906.5) (Ha et al., 2019; Manzulli et al., 2021).

Regarding the processing of the investigated replicates for the bacterial isolates, the recorded mass spectra suggest that, in many cases, we may be dealing with different strains of the same species (examples are shown in **Figure II.3.4**). Detailed investigations of the white bacterial colony B_{11} (collected at Building A, ~1 m above ground level) revealed signals specific to surfactin C and surfactin D. **Figure II.3.6** presents MS and MS/MS spectra acquired in positive-ion mode using the MALDI–Orbitrap MS tandem setup. For the m/z 1036.7 precursor, the MS/MS spectrum was recorded using 30% collision energy and an isolation window of 3 m/z.

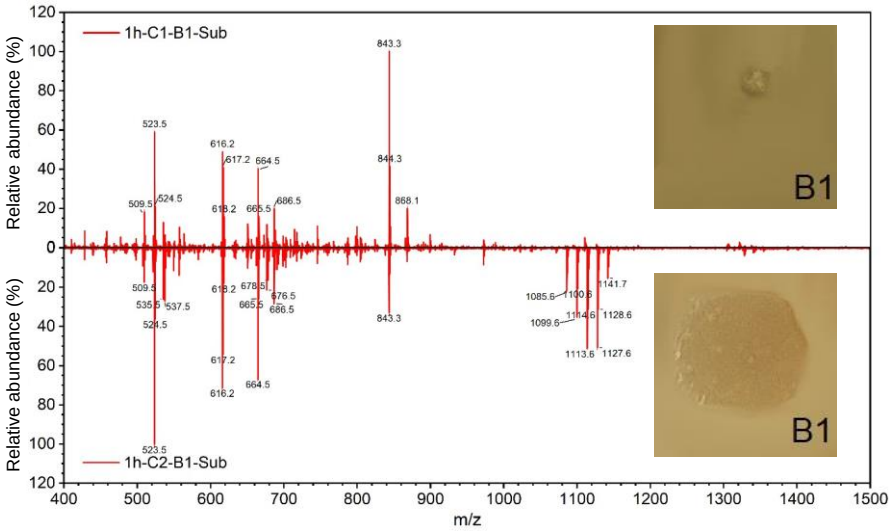

Moderate similarity between white bacterial colonies (B_{12} and B_{14}) identified in replicate samples from Building C, ~35 m above ground level

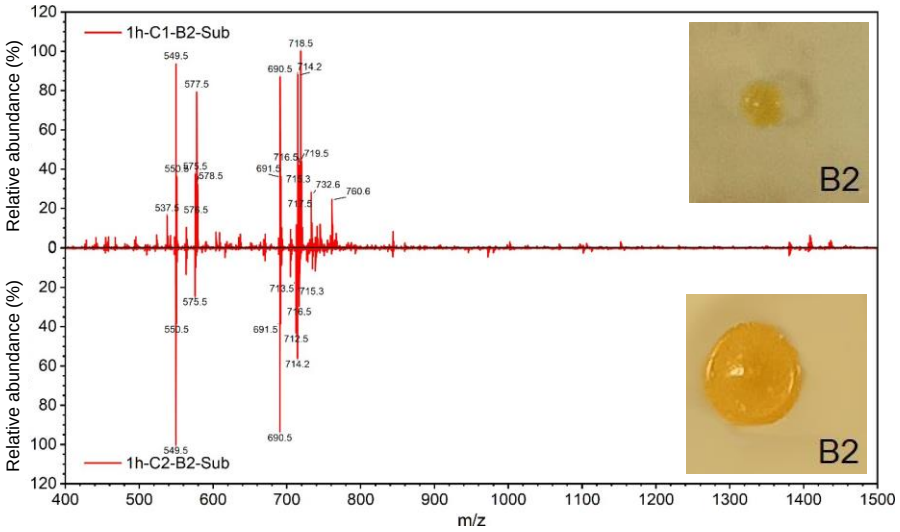

Good similarity between white bacterial colonies (B_{22} and B_{24}) identified in replicate samples from Building C, ~35 m above ground level

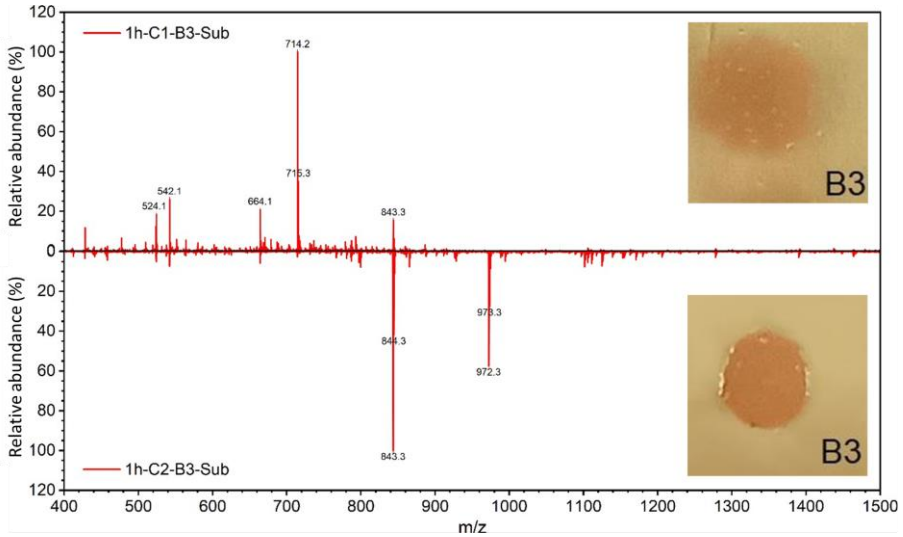

Low similarity between white bacterial colonies (B_{32} and B_{34}) identified in replicate samples from Building C, ~35 m above ground level

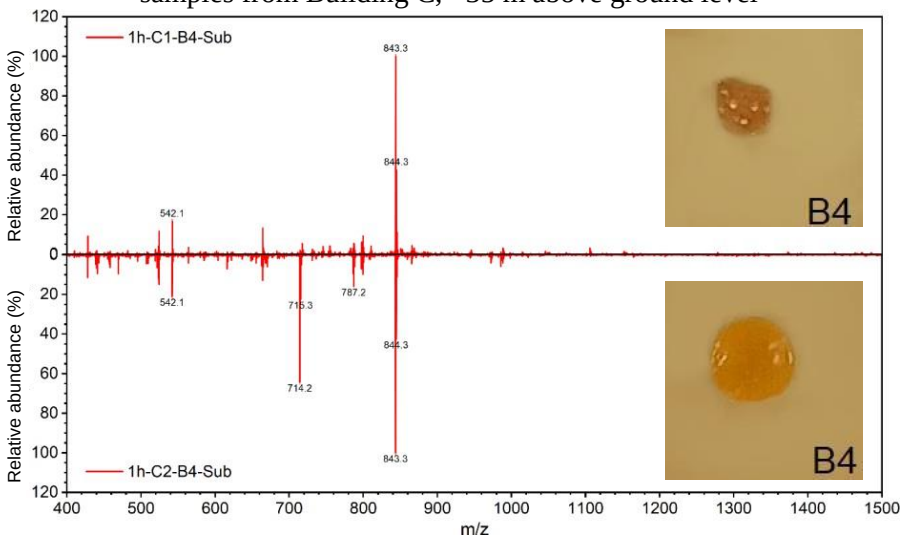

Good similarity between white bacterial colonies (B_{42} and B_{44}) identified in replicate samples from Building C, ~35 m above ground level

Figure II.3.4: Mass spectra in the m/z 400–1500 range for bacterial sample replicates after subtraction of the matrix and blank signals.

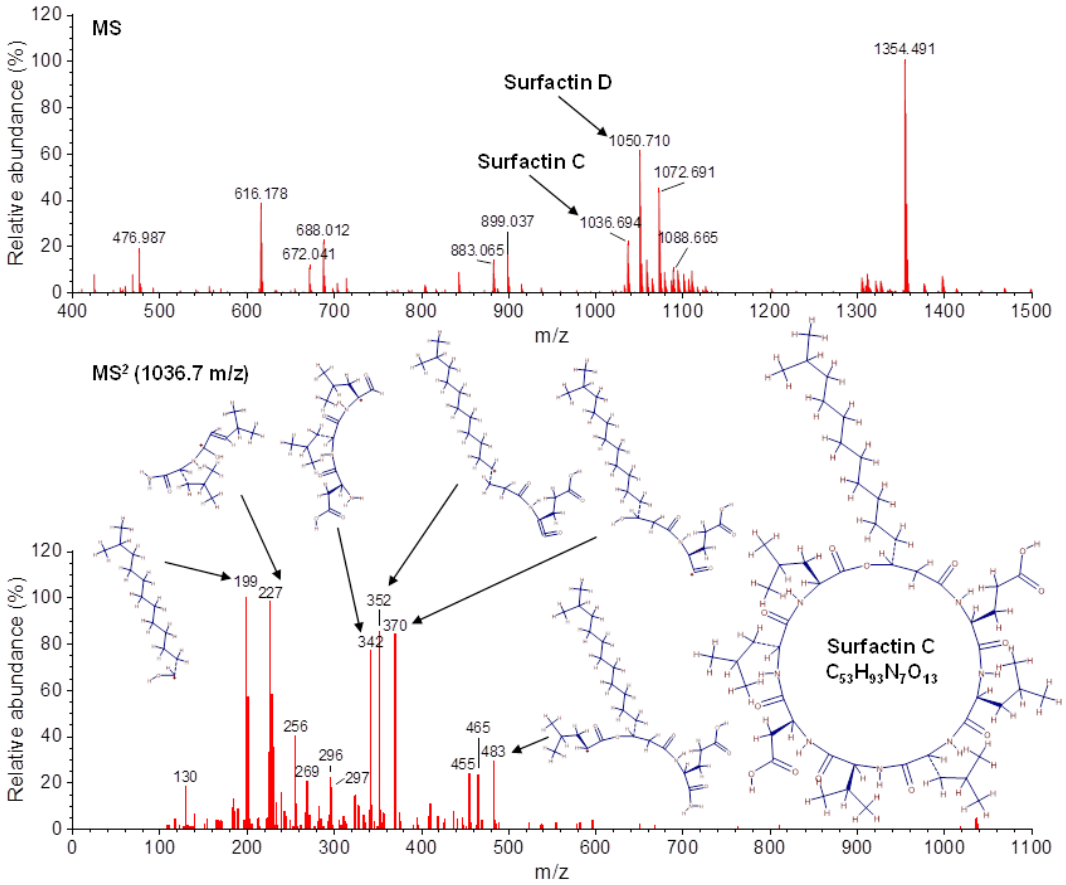

Figure II.3.6: MS and MS/MS spectra acquired in positive-ion mode using MALDI–Orbitrap MS for surfactin C and surfactin D.

The isotopic evaluation results confirm the molecular formula of surfactin C (molecular ion $[C_{53}H_{93}N_7O_{13} + H]^+$) and surfactin D (molecular ion $[C_{54}H_{95}N_7O_{13} + H]^+$) in the bacterial colony B_{11} present in samples collected at 1 m above ground level. For the fungal samples, the species denoted F1 exhibited distinct spectral profiles among the replicates from Building A, whereas the replicates from Building C were characterised by spectra with relatively similar profiles (**Figure II.3.7**).

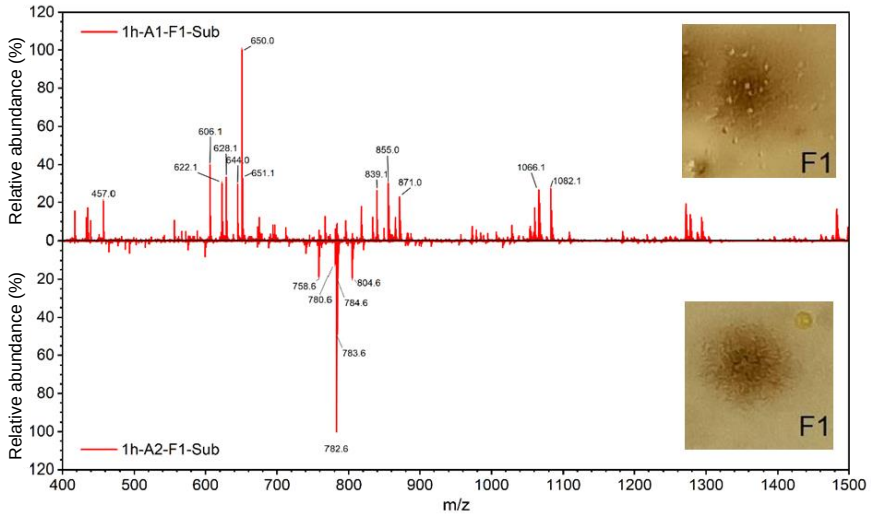

(a)

Extremely low similarity among fungal colonies identified in replicates from Building A, ~1 m above ground level (brown fungal colonies).

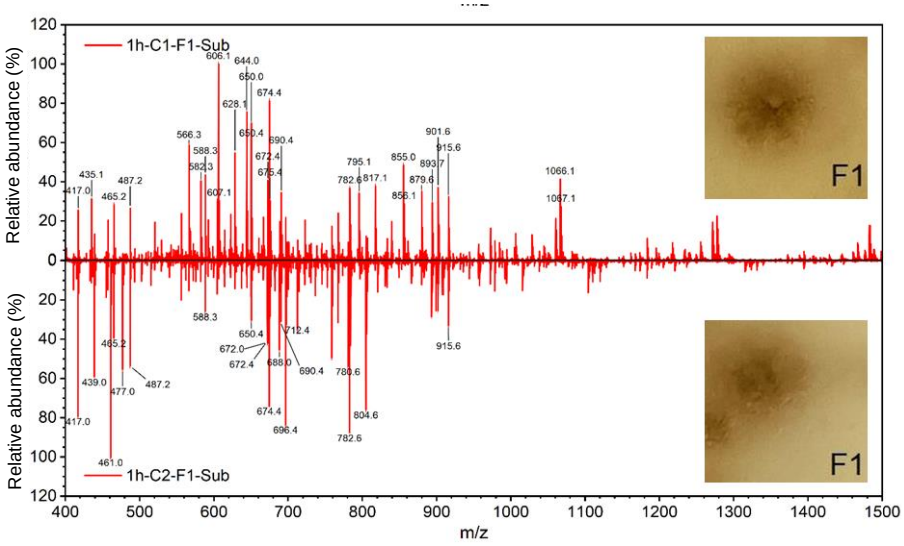

(b)

Moderate similarity among fungal colonies identified in replicates from Building C, ~35 m above ground level (brown fungal colonies).

Figure II.3.7: Mass spectra (m/z 400–1500) for fungal samples after subtraction of the sample matrix and blank signals.

Very similar spectra were observed for the fungal colony denoted F3, both among replicates and between colonies originating from the two sampling locations (**Figure II.3.7**). In this study, MALDI–Orbitrap MS analyses highlighted relevant features of microorganisms isolated from urban particulate matter in Iasi, although structural assignments were only possible for a limited number of compounds. A more in-depth evaluation remains the subject of future research. The technique is rapid and generally reliable for phenotypic identification; however, it has certain limitations.

II.3.2 Determination of elemental concentrations in microorganisms isolated from ambient particulate matter using ICP-MS

The elemental composition of particulate matter-borne bioaerosols from Iasi was determined by ICP-MS for both essential and toxic elements. The analyses targeted microorganisms isolated and purified from bioaerosols associated with the 24 April 2024 event. The isolates (bacteria, fungi, and yeasts) obtained by passive sampling were taxonomically identified to genus/species level in the laboratories of Eurofins BIOMI Ltd. (Hungary) prior to ICP-MS determinations. For the 4 bacteria, 5 fungi, and 2 yeasts, the codes used here correspond to those in **Table II.2.7**.

II.3.2.1 Sample preparation procedure for the quantitative transfer into solution of microorganisms isolated from bioaerosols associated with ambient particulate matter from the urban area of Iasi

For ICP-MS analysis, bacterial, fungal, and yeast isolates were cultured until sufficient biomass was obtained for quantitative determination. For each microorganism, triplicates were prepared by growth for ≥24 h on Luria–Bertani medium (bacteria and yeasts) and Sabouraud medium (fungi). From each culture, 24–173 mg of material were carefully collected while minimising carry-over of the culture medium, after which the samples were mineralised/digested.

For the microorganisms $B_{Pri.\ ary.}$, $F_{Alt.\ des.}$, $F_{Alt.\ sp.}$, $F_{Cla.\ sp.\ 1}$, and $F_{Cla.\ sp.\ 2}$, one replicate out of three was excluded due to limited biomass development. Quantitative transfer of analytes into solution was achieved by microwave-assisted digestion, using a SpeedWave Xpert system with a DAP40 rotor (24 vessels, two rows; Analytik Jena, Germany). The rapid and

straightforward programme was derived from EPA 3052 (U.S. EPA, 1996). After digestion, the samples were filtered through Whatman® Grade 41 filter paper (Merck) and made up to 10 mL with ultrapure water produced by an OmniaPure UV/UF-TOC system (StakPure, Germany). Complete dissolution was visually confirmed during the filtration step illustrated in **Figure II.3.8**, which presents the sequence of preparative and analytical steps.

Figure II.3.8: Sample preparation steps, including microwave-assisted digestion, prior to metal-content determination by ICP-MS.

II.3.2.3 Total concentrations of the analysed metallic species in microorganisms isolated from bioaerosols associated with ambient particulate matter

The mean elemental abundance in the samples follows the order: Ca > Mg > Al > Zn > Fe > Mn > Sr > B > Rb > Ba > Cu > Cr > V > Pb > Tl > Mo > Li > Ni > Co > Cd > Bi > U. **Table II.3.5** reports the mean concentrations (± absolute uncertainty) for elements at the µg g^{-1} level (**Table II.3.5a)** and the ng g^{-1} level (**Table II.3.5b**). **Figure II.3.10** shows, as radial plots, elements with potential cellular roles (Fe, Cu, Zn, Ni, Co, Mn, V), together with the sum of Ca, Mg, Al, B, Rb, Sr, and Ba, and the ultra-trace elements (sum of Cr, Pb, Tl, Li, Cd, Bi, U). According to **Table II.3.5**, Ca and Mg are the most abundant; Ca reaches its highest value in the $B_{Pri.\ ary.}$ colony, which also exhibited the most pronounced proliferation within the first 12 h of incubation. Mg and Cr attain the highest values across all bacterial colonies, without a clear pattern in fungi and yeasts. Al, Zn, Fe, Mn, Ba, Cr, V, Ni, Mo, Li, Cd, and Co show higher abundances in $B_{Pla.\ wig.}$ and $B_{Pri.\ ary.}$ than in $B_{Agr.\ cit.}$, with no specific trend in the fungal/yeast isolates.

Although **Table II.3.5** reports total concentrations, a substantial fraction may occur as readily bioavailable ionic forms involved in signalling, catalysis, or structural roles. **Figure II.3.10** highlights essential transition metals (Fe, Zn, Mn, Cu, Ni, Co) at low levels, with key catalytic functions in microbial metabolism (Pernil and Schleiff, 2019).

Many elements (Fe, Cu, Zn, Ni, Mn, Mo, Co, V) are commonly utilised by microorganisms, whereas the presence of potentially toxic species such as Cr, Pb, and U in isolates from urban particles in Iasi is likely related to pollution exposure during air-mass transport.

Table II.3.5: Estimated concentrations of the elements identified in bacteria (B), fungi (F), and yeasts (D) isolated from ambient PM in the urban area of Iasi.

a	**trace elements (µg g^{-1})**										
Sample	Ca	Mg	Al	Zn	Fe	Mn	B	Sr	Rb	Ba	Cu
$B_{Pla.\ wig}$	376 ± 8	197 ± 5	27.6 ± 1.1	15.9 ± 0.5	27.6 ± 2	5.51 ± 0.20	0.30 ± 0.02	1.64 ± 0.07	1.59 ± 0.05	1.32 ± 0.04	0.18 ± 0.01
$B_{Pri.\ ary.}$	2031 ± 27	190 ± 3	59.7 ± 1.4	20.7 ± 0.4	19.8 ± 0.4	4.53 ± 0.13	0.40 ± 0.01	4.41 ± 0.09	0.71 ± 0.01	1.82 ± 0.06	0.20 ± 0.01
$B_{Agr.\ cit.}$	255 ± 5	172 ± 5	0.9 ± 0.2	8.8 ± 0.2	7.6 ± 0.6	1.78 ± 0.07	0.37 ± 0.02	1.25 ± 0.04	1.61 ± 0.05	0.77 ± 0.03	0.35 ± 0.02
F_{Fus}	191 ± 6	182 ± 9	10.5 ± 0.4	17.7 ± 0.5	7.9 ± 0.4	0.86 ± 0.03	0.53 ± 0.02	1.31 ± 0.04	0.83 ± 0.02	0.39 ± 0.04	0.41 ± 0.03
$F_{Alt.\ des.}$	100 ± 1	28 ± 1	8.0 ± 0.2	1.6 ± 0.1	1.3 ± 0.1	0.20 ± 0.01	3.03 ± 0.11	0.51 ± 0.02	0.51 ± 0.01	0.10 ± 0.01	0.29 ± 0.01
$F_{Alt.\ sp.}$	156 ± 5	142 ± 2	24.1 ± 0.6	18.4 ± 0.2	12.7 ± 0.5	0.34 ± 0.01	0.97 ± 0.03	1.10 ± 0.04	0.48 ± 0.01	0.54 ± 0.01	0.27 ± 0.01
$F_{Cla.\ sp.1}$	502 ± 13	55 ± 1	8.7 ± 0.1	4.4 ± 0.1	4.1 ± 0.9	0.52 ± 0.02	5.59 ± 0.06	2.12 ± 0.05	1.22 ± 0.03	0.64 ± 0.02	0.28 ± 0.01
$F_{Cla.\ sp.2}$	155 ± 3	20 ± 1	2.5 ± 0.1	1.1 ± 0.1	n.d.	0.14 ± 0.01	1.40 ± 0.05	0.81 ± 0.04	0.42 ± 0.01	0.20 ± 0.01	0.06 ± 0.01
$D_{Aur.\ sp.\ 1}$	247 ± 19	64 ± 1	n.d.	24.7 ± 0.6	7.3 ± 1.8	2.38 ± 0.06	0.76 ± 0.03	0.66 ± 0.03	0.74 ± 0.03	0.42 ± 0.03	n.d.
$D_{Aur.\ sp.\ 2}$	232 ± 4	47 ± 1	1.6 ± 0.1	8.2 ± 0.3	4.0 ± 1.0	1.33 ± 0.08	n.d.	0.72 ± 0.03	0.16 ± 0.01	0.46 ± 0.01	0.19 ± 0.02
b	**ultra-trace elements (ng g^{-1})**										
Sample	Cr	V	Pb	Ni	Tl	Li	Mo	Cd	Co	Bi	U
$B_{Pla.\ wig}$	315 ± 13	131 ± 18	77 ± 4	30.3 ± 2.0	38.7 ± 3.0	70.8 ± 6.3	85.7 ± 7.3	28.2 ± 6.3	22.0 ± 2.8	6.4 ± 0.9	0.60 ± 0.16
$B_{Pri.\ ary.}$	288 ± 9	120 ± 8	410 ± 8	84.7 ± 0.1	102.5 ± 5.0	71.3 ± 0.5	66.5 ± 2.8	39.9 ± 10.1	34.5 ± 1.1	11.1 ± 2.1	1.19 ± 0.33
$B_{Agr.\ cit.}$	201 ± 9	92 ± 10	113 ± 5	13.1 ± 0.7	115.0 ± 2.4	26.0 ± 2.6	3.3 ± 1.7	9.9 ± 4.0	5.0 ± 0.4	4.7 ± 0.8	0.29 ± 0.02
F_{Fus}	92 ± 5	87 ± 7	11 ± 1	9.0 ± 0.3	8.3 ± 1.7	11.0 ± 1.3	41.0 ± 3.3	17.0 ± 11.9	8.3 ± 1.2		0.38 ± 0.12
$F_{Alt.\ des.}$	86 ± 3	130 ± 6	14 ± 1		6.5 ± 1.4	7.3 ± 0.9	20.0 ± 2.2		10.2 ± 1.6		2.52 ± 0.34
$F_{Alt.\ sp.}$	73 ± 1	78 ± 7	13 ± 1	12.5 ± 1.1	4.5 ± 1.4	14.3 ± 1.4	21.5 ± 1.4	25.0 ± 6.1	10.2 ± 0.4		0.79 ± 0.14
$F_{Cla.\ sp.1}$	221 ± 4	320 ± 9	47 ± 1	84.1 ± 0.1	17.0 ± 1.4	10.2 ± 1.1	42.0 ± 2.2		19.6 ± 0.5	1.7 ± 0.3	3.91 ± 0.42
$F_{Cla.\ sp.2}$		53 ± 4	22 ± 1		8.5 ± 1.4	6.7 ± 1.2	11.0 ± 1.4		30.8 ± 4.1		1.79 ± 0.39
$D_{Aur.\ sp.\ 1}$	85 ± 2	115 ± 13	93 ± 6		25.0 ± 3.7	78.3 ± 9.1	24.5 ± 3.2				1.55 ± 0.19
$D_{Aur.\ sp.\ 2}$	94 ± 3	88 ± 6	68 ± 2			44.1 ± 2.8	18.5 ± 1.4				9.72 ± 0.26

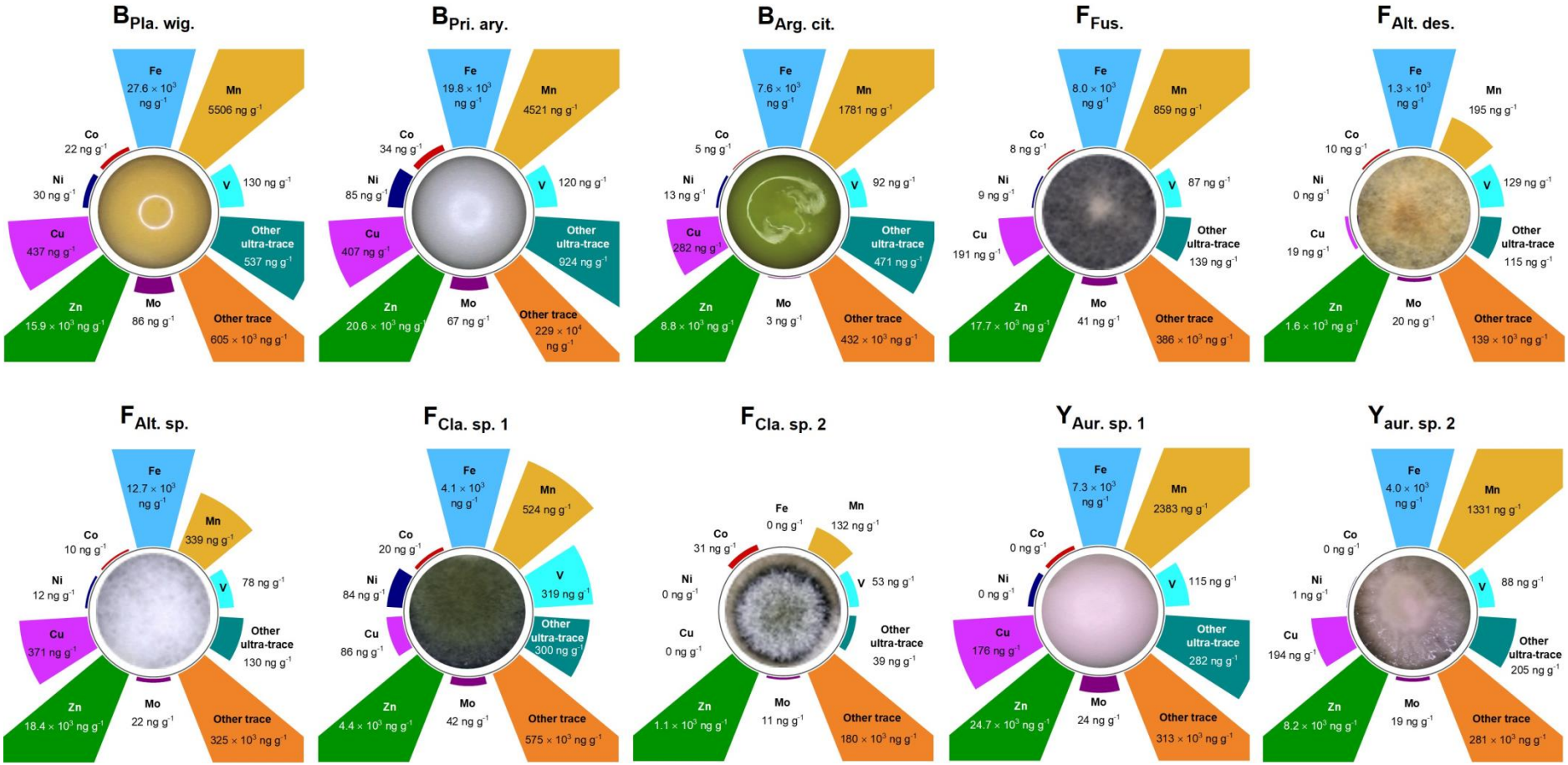

Figure II.3.10: Radial plots of the distribution of essential elements with potential cellular relevance, together with the contributions of other elements at trace and ultra-trace concentration levels.

II.4 ANALYSIS OF GASEOUS COMPOUNDS EMITTED BY MICROORGANISMS ISOLATED FROM BIOAEROSOLS ASSOCIATED WITH AMBIENT PARTICULATE MATTER USING SELECTED ION FLOW TUBE MASS SPECTROMETRY (SIFT-MS)

II.4.1 Sample preparation and measurements

Samples for SIFT-MS were collected by passive settling onto Petri dishes containing LB and SAB agar at the AMOS station on 24 April 2024, between 16:00 and 19:00, as described in **Chapter II.2.1**. For the analysis of VOCs emitted by the isolated microorganisms (bacteria, fungi, yeasts) from the bioaerosol fraction, Restek polypropylene bags were used, with the outlet airflow monitored using the same technology.

After incubation, colonies were isolated and purified on nutrient agar plates and then transferred into Restek bags. The bags were heat-sealed, residual air was removed using a vacuum pump, and they were subsequently filled with synthetic air to a volume of 400 mL. The workflow is illustrated in **Figure II.4.1.**

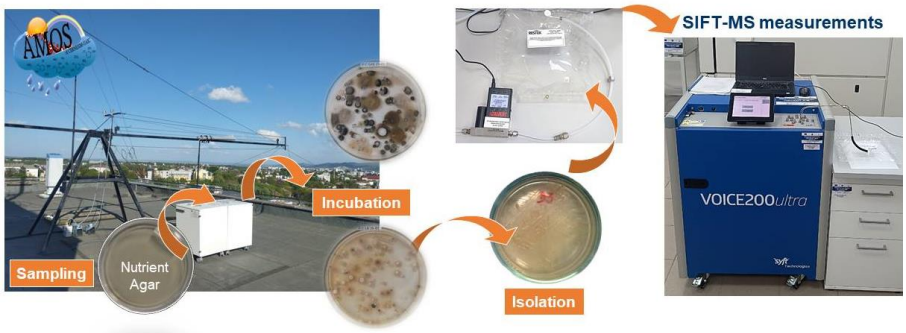

Figure II.4.1: Schematic overview of the steps followed for SIFT-MS analysis of gaseous compounds emitted by microorganisms isolated from atmospheric bioaerosols.

The composition of the gas mixture was monitored by SIFT-MS immediately after inoculation (time zero), after which the samples were incubated at 28 °C and analysed at 2, 4, 6, 8, 24, 26, 28, and 30 h; after each measurement, the bags were refilled with synthetic air to the same volume.

As blanks/controls, bags containing only Petri dishes with culture media were included and maintained under the same conditions; sampling was performed at a constant flow rate of 24 mL min^{-1}.

Acquisition spectra were recorded in positive-ion mode over the m/z 15–250 range, at unit mass resolution, with 10 cycles per measurement, using H_3O^+, NO^+, and O_2^+ as reagent ions. The SIFT-MS instrument was calibrated using a reference gas mixture (Syft Technologies) containing benzene, p-xylene, ethylene, isobutane, 1,2,3,4-tetrafluorobenzene, perfluorobenzene, toluene, and octafluorotoluene.

II.4.2 Study of volatile compounds emitted during the development of microorganisms isolated from airborne bioaerosols in the urban area of Iasi

Volatile compounds emitted by microorganisms can generate characteristic profiles that are useful for their identification or investigation using rapid and sensitive analytical methods applicable across a wide range of applications (Garcia-Alcega et al., 2017; Roslund et al., 2020; Reese et al., 2020). Bacteria, yeasts, and fungi release various classes of compounds-particularly alcohols, ketones, aldehydes, acids, phenolic compounds, and sulfides (El Jaddaoui et al., 2023; Ling et al., 2022; Zhang et al., 2022).

The ions observed at m/z 37, 55, and 73 under H_3O^+ conditions originate from H_3O^+ with water-cluster ions; those at m/z 30 and 48 for NO^+ result from NO^+ with water-clustering; and ions at m/z 32, 37, and 55 in O_2^+ mode may reflect minor H_3O^+ impurities generated during O_2^+ formation. The compounds investigated in emissions from bacteria, fungi, and yeasts isolated from bioaerosols in the urban atmosphere of Iasi are summarised in **Table II.4.1**.

Table II.4.1: Primary product ions together with their m/z ratios, including water adducts, used to investigate the compounds reported in the present study (m/z values of isotopes showing significant signals in the mass spectra are given in parentheses).

Compound	MF	Reagent ion		
		H_3O^+	NO^+	O_2^+
acetaldehyde	C_2H_4O	45, 63, 81	43, 74, 61	43, 44
ethyl acetate	$C_4H_8O_2$	89, 107	118	
acetone	C_3H_6O	59, 77, 95, 117	88	43, 58
acetonitrile	C_2H_3N	42, 60, 78, 96, 83	71 (72)	
acetic acid	$C_2H_4O_2$	61, 79, 97	90, 108	43, 60
lactic acid	$C_3H_6O_3$	91		
ammonia	NH_3	18, 36, 54	-	17, 35
butanone	C_4H_8O	73*, 91, 145	102	43, 57, 72, 73
etthyl butyrate	$C_6H_{12}O_2$	117		
hydrocyanic acid	HCN	28, 46, 64		
dimethylsulphide	C_2H_6S	63 (65)	62	
dimethyldisulphide	$C_2H_6S_2$	95 (97)	94 (96)	94 (96)
dimethyltrisulphide	$C_2H_6S_3$	127 (129)		
ethanol	C_2H_5OH	47, 65, 83, 93, 111	45, 63, 81	
ethyl-pyrazine	$C_6H_8N_2$	109		
hydrogen sulfide	H_2S	35, 53	-	-
indole	C_8H_7N	118	117	
isoprene	C_5H_8	69	68	
methanol	CH_3OH	33, 51, 69, 83	62	31, 32
methanethiol	CH_4S	49, 67, 85	-	
methyl-pyrazine	C_5H_6N	95		
methylthio-acetate	C_3H/OS	91		
propanol	C_3H_7OH	43, 61, 79, 97	59, 77, 119	31,42,59
trimethylamine	C_3H_9N	60	59	58, 59

1-(methylthio)-3-pentanone	$C_6H_{12}OS$	133		
2-amino-acetophenone	C_8H_9NO	136		
2-phenylethanol	$C_8H_{10}O$	123		

To verify the correct assignment of chemical species, multiple signals in the mass spectra that can be attributed to the same compound were used and treated as variables of interest. For example, for ammonia, the signals at m/z 18 and m/z 36 can be used, corresponding to NH_4^+ and NH_3^+ (H_2O), respectively, in the ionisation mode employing H_3O^+ as the precursor (reagent) ion (**Figure II.4.4a**).

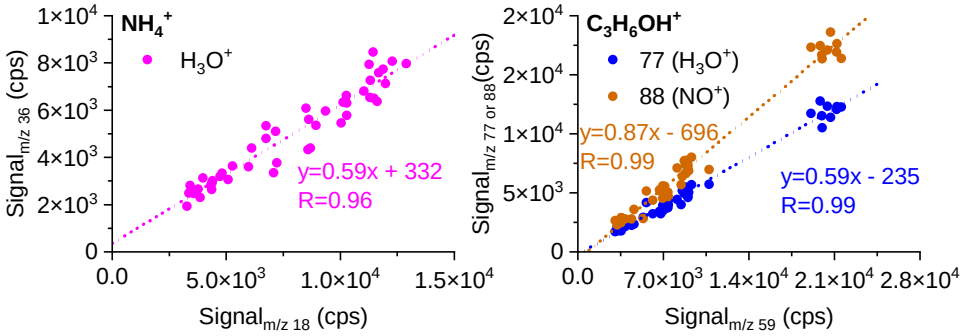

(a) **(b)**

Figure II.4.4: Assessment of signal assignment using regression analysis of multiple signals for ammonia **(a)** and acetone **(b)** when employing H_3O^+ and NO^+ precursor (reagent) ions for a single dataset.

For acetone, the signals at m/z 59, 77, and 88 were monitored: the primary product ion and the hydrated secondary product ion in H_3O^+ mode, and the primary product ion in NO^+ mode (**Figure II.4.4b**).

To discriminate signals specific to emissions from bacteria, fungi, and yeasts, the composition of the synthetic air used to control growth conditions and the contributions originating from the culture media were analysed; representative mass spectra for these measurements are shown in **Figure II.4.5**.

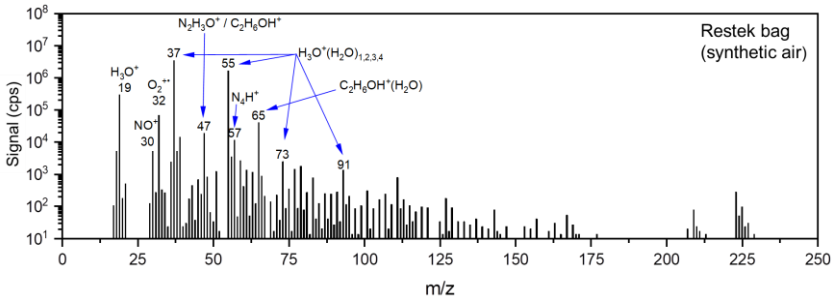

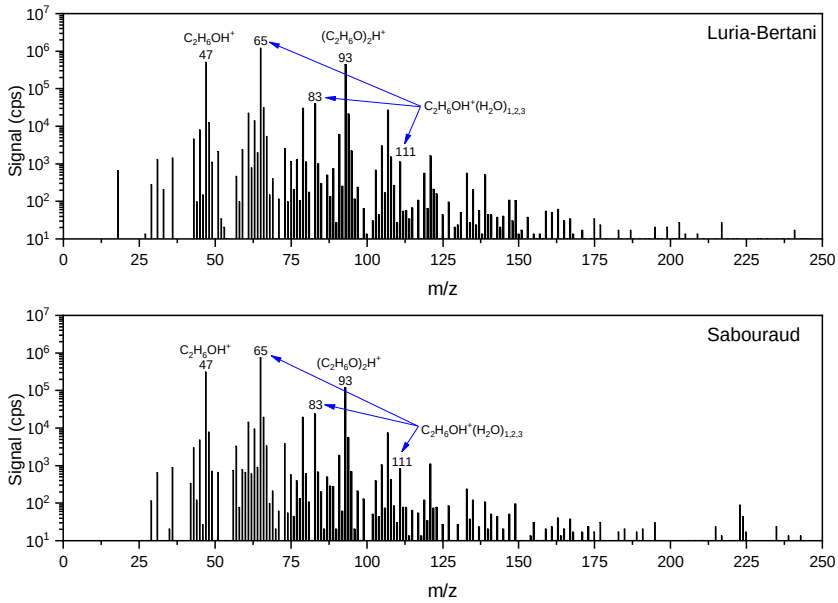

Figure II.4.5: Representative mass spectra acquired in the ionisation mode using H_3O^+ as the reagent (precursor) ion for the synthetic air and the culture media used for microbial growth, Luria-Bertani and Sabouraud.

Microbial growth was initially monitored at 2 h intervals during the first 8 h of incubation, and after 30 h satisfactory abundances of the investigated species were obtained in the mass spectra; therefore, the data presented for bacteria, fungi, and yeasts correspond to this time point. **Figure II.4.6** illustrates the SIFT-MS spectra acquired using H_3O^+ reagent ions for emissions from the isolated bacteria after 30 h of incubation; for the isolated fungi, the corresponding results are shown in **Figure II.4.7**.

For the bacterial isolates, the following compounds were evidenced: ammonia at m/z 18 and 36 for *Planococcus wigleyi* and *Agrococcus citreus*; acetaldehyde at m/z 45 for *P. aryabhattai*; acetone at m/z 59 and 77 for *P. wigleyi* and *P. aryabhattai*; 2-butanone at m/z 91 (water adduct) for *P. aryabhattai*; as well as weak p-xylene signals at m/z 106 for *P. aryabhattai* and *A. citreus*.

For the fungal isolates, *Cladosporium* sp. and *Alternaria destruens* showed acetone signals at m/z 77, whereas the *Fusarium* sp. isolate generated intense signals for acetaldehyde (m/z 63), ethanol (m/z 93), and butanone (m/z 73 and 91). In more detail, ions at m/z 135/137 and 151/153 may be associated with monoterpenes, while acetic acid and acetone were identified via product ions at m/z 61 and 59, respectively. Ions at m/z 117, 77, and 81 may arise from monoterpene fragmentation in the ionisation flow tube.

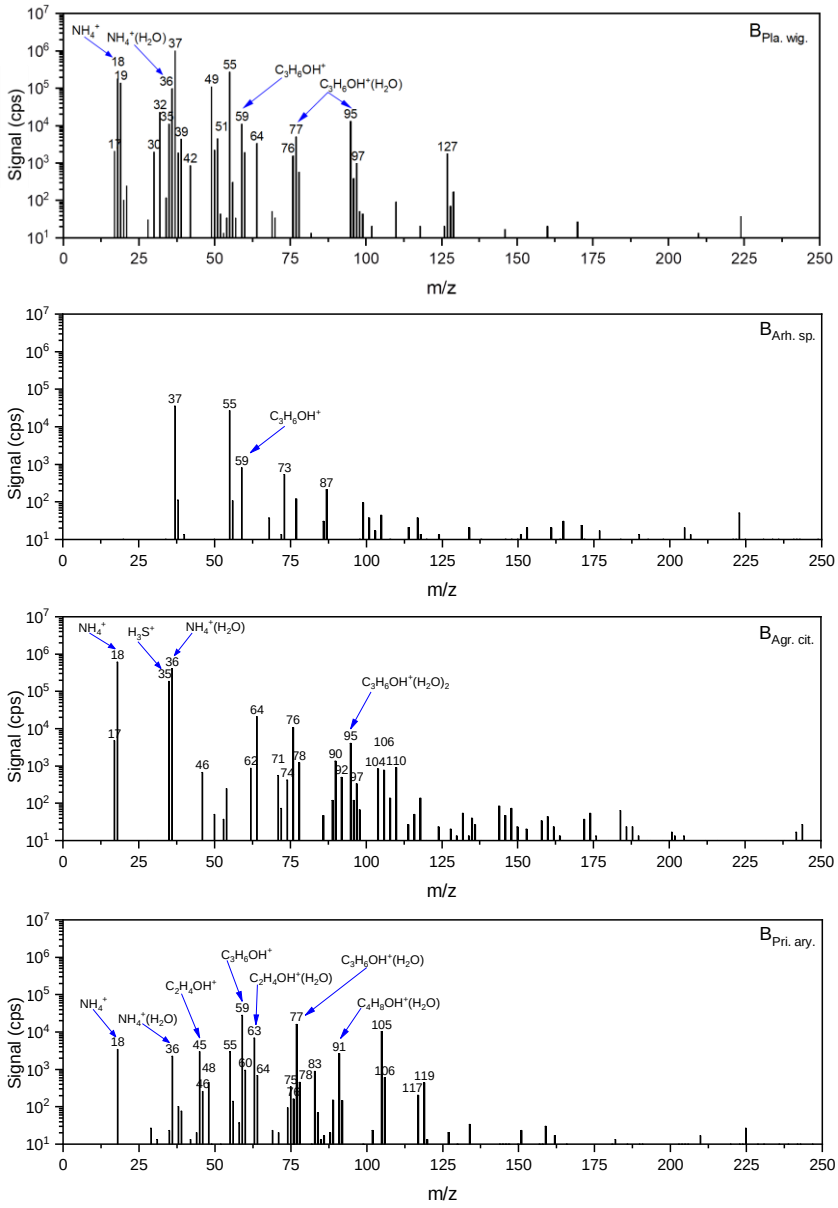

Figure II.4.6: Representative mass spectra acquired in the ionisation mode using H_3O^+ as the reagent (precursor) ion for the isolated bacteria (*Planococcus wigleyi*, *Priestia aryabhattai*, *Agrococcus citreus*, *Arthrobacter* sp.) after 30 h of incubation.

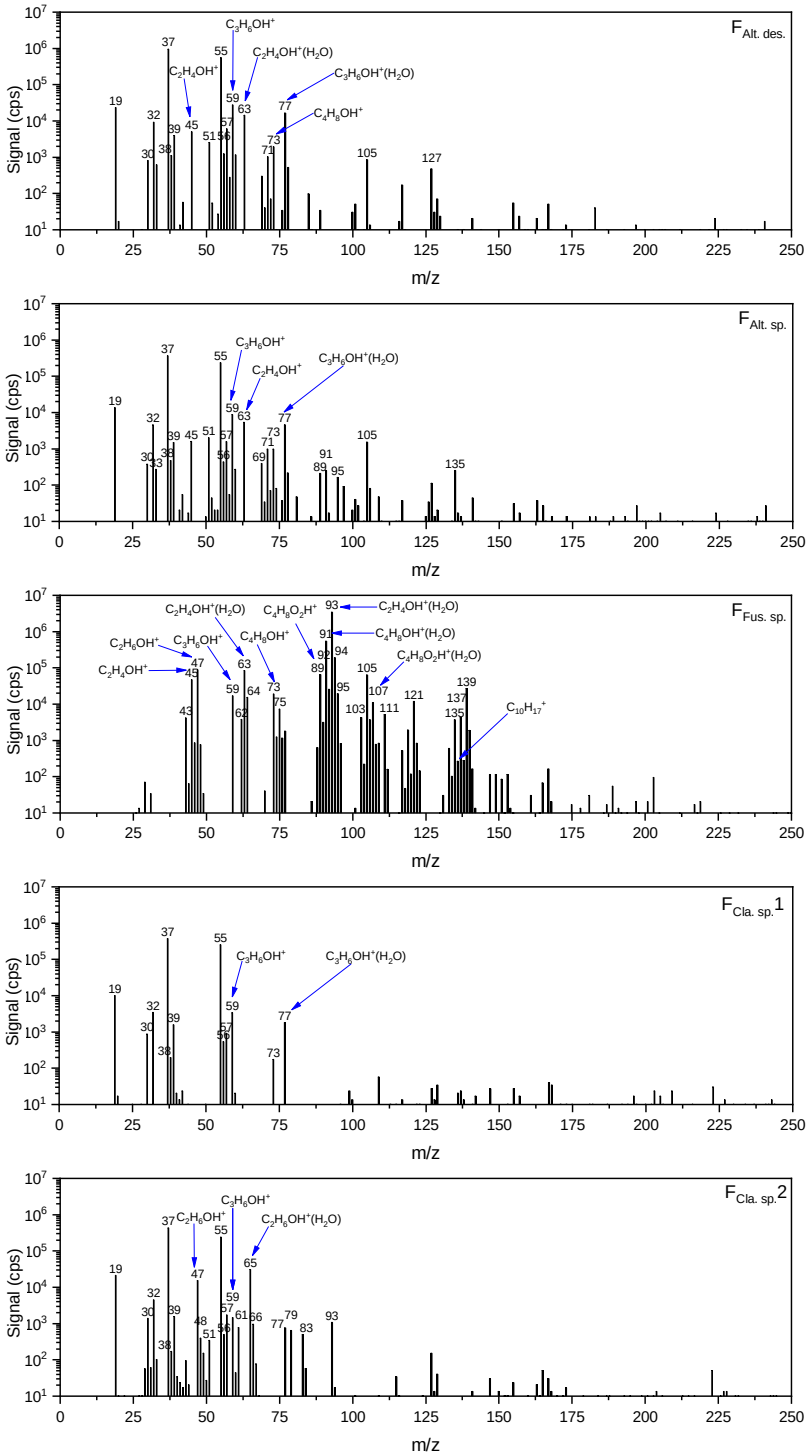

Figure II.4.7: Representative mass spectra acquired in the ionisation mode using H_3O^+ as the reagent (precursor) ion for the isolated fungi (*Fusarium*, *Alternaria destruens*, *Cladosporium sp.*) after 30 h of incubation.

Table II.4.2 presents the results associated with the Venn-diagram analysis, operationalised using data derived from the mean mass spectra of the samples after subtraction of the blank/control contributions. Signals with post-subtraction intensities greater than 100 cps were used. Samples were grouped by species because the maximum number of cases that can be included in this analysis is 6. Accordingly, three groups were obtained, as shown in **Table II.4.2.**

Table II.4.2: Results of the Venn-diagram analysis of the spectral data for fungi, bacteria, and yeasts isolated from bioaerosols associated with particulate matter in the urban atmosphere of Iasi.

Fungi

00101	*01000*	*01101*	*01111*	*10000*		*10001*	*10100*	*10101*	*11000*	*11111*
33	49	51	38	43	111	89	117	45	48	59
60	61	127	39	46	112	95		63	93	77
69	66		56	62	119	135		105		
71	79			64	120					
78	83			74	121					
				75	122					
				76	123					
				88	133					
				90	136					
				92	137					
				94	138					
				96	139					
				103	140					
				104	141					
				106	147					
				107	149					
				108	153					
				109	167					

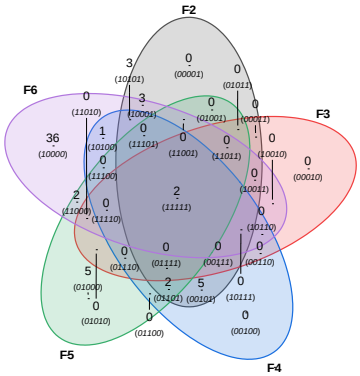

Bacteria

0001	*0010*	*0100*	*0101*	*0111*	*1000*	*1001*	*1100*	*1101*
34	87	45	60	59	54	35	46	18
42		48		77	62	95	89	36
49		63			71	96	92	64
50		75			74	97	106	76
51		83			90			78
127		105			104			
129		117			108			
		119			110			
					118			

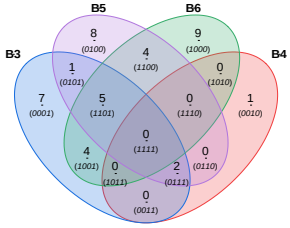

Yeast

01	*10*	*11*
35	45	18
42	48	36
59	63	46
76	83	60
77	87	74
78	127	
110		
117		

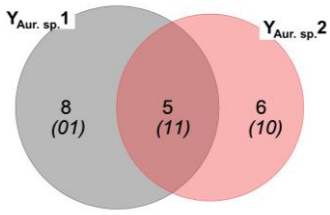

Comparative analysis shows that all bacteria, except *A. citreus*, emitted acetone (m/z 59, 77); *P. wigleyi* and *P. aryabhattai* shared trimethylamine (m/z 60); and all bacteria, except *Arthrobacter* sp., emitted ammonia (m/z 18, 36). Among sulfur-containing species, H_2S (m/z 35) and dimethyl sulfide (m/z 95, 96, 97) were identified for *P. wigleyi* and *A. citreus*. Distinctly for *P. aryabhattai*, acetaldehyde (m/z 45, 63) was observed, whereas for *P. wigleyi* acetonitrile (m/z 42), methanethiol (m/z 49), and dimethyl trisulfide (m/z 127, 129) were noted.

For fungi, emissions of volatile compounds are generally lower than for bacteria and yeasts; however, *Fusarium* sp. exhibited a considerable number of signals (36 m/z values), and *Cladosporium* sp.2 also showed distinct signals (5 m/z values). For yeasts, acetaldehyde (m/z 45, 63) was common; for *Aureobasidium* sp.1, acetone (m/z 59, 77) and H_2S (m/z 35) were distinctive, whereas for *Aureobasidium* sp.2 ammonia (m/z 18, 36) was distinctive.

Factor analysis yielded a four-factor solution (Figure II.4.9) explaining a cumulative variance of 93%, with the first factors accounting for 72.5% of the total variance.

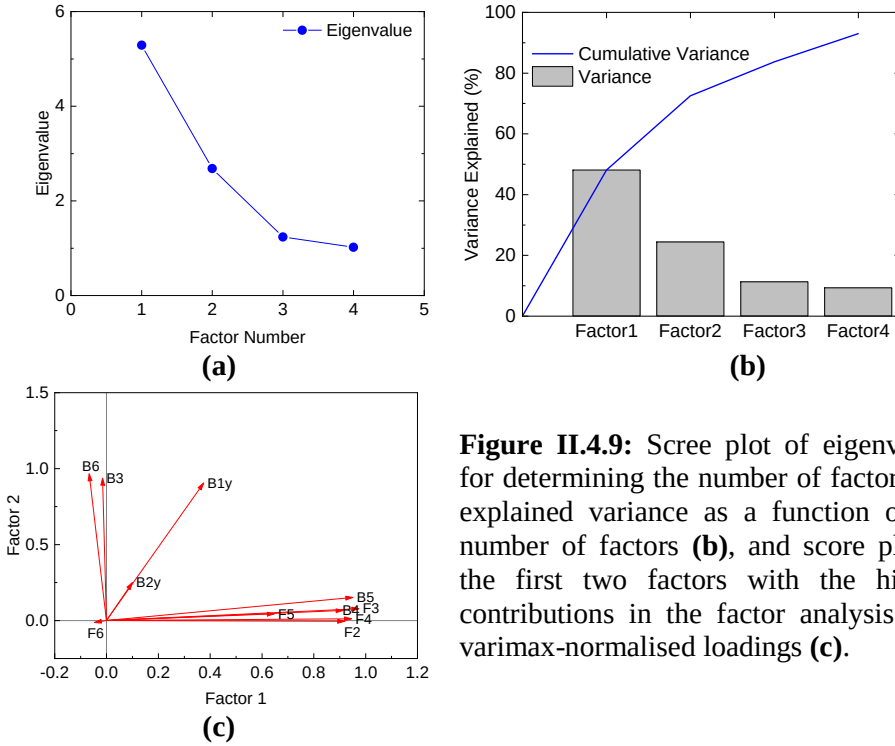

Figure II.4.9: Scree plot of eigenvalues for determining the number of factors **(a)**, explained variance as a function of the number of factors **(b)**, and score plot of the first two factors with the highest contributions in the factor analysis with varimax-normalised loadings **(c)**.

For the factor analysis, mean spectra obtained after 30 h of incubation were used, after subtraction of the blank/control signals. Factor 1 groups the fungi together with the bacteria *Arthrobacter* sp. ($B_{Arh.sp.}$) and *P. aryabhattai* ($B_{Pri.ary.}$), whereas *Fusarium* sp. ($F_{Fus.sp.}$) is separated into Factor 3. Factor 2 is

represented by *Aureobasidium* sp.1 ($B_{Aur.sp.1}$), *P. wigleyi* ($B_{Pla.wig.}$), and *A. citreus* ($B_{Agr.cit.}$), while *Aureobasidium* sp.2 ($B_{Aur.sp.2}$) is separated into Factor 4.

According to **Figure II.4.10**, the acetone-emission profiles of the fungi indicate a more pronounced increase for *A. destruens* ($F_{Alt.des.}$) and *Fusarium* sp. ($F_{Fus.sp.}$), with a marked rise in concentrations after approximately 6 h of incubation.

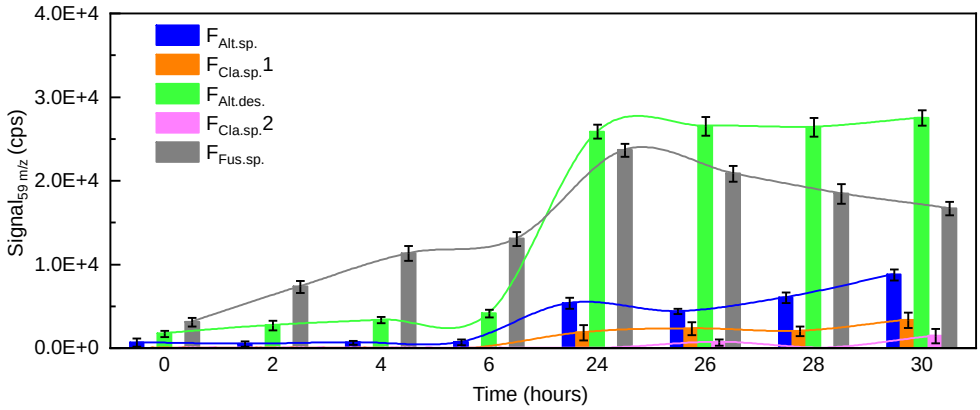

Figure II.4.10: Temporal profile of the acetone signal (m/z 59) measured in emissions from the five fungal isolates obtained from bioaerosols associated with ambient particulate matter in the city of Iasi.

For *Fusarium* sp. ($F_{Fus.sp.}$), a decrease in acetone abundance was observed after 24 h, whereas for *A. destruens* ($F_{Alt.des.}$) the abundance remained constant. For the bacterial culture *P. wigleyi*, elevated signals at m/z 49 (methanethiol, protonated CH_4S), m/z 95 (dimethyl disulfide, protonated $C_2H_6S_2$), and m/z 127 (dimethyl trisulfide, protonated $C_2H_4S_3$) were observed, indicating emissions of sulfur-containing compounds. **Figure II.4.11** describes the temporal evolution of these sulfur compounds for *P. wigleyi* (BPla.wig.): increased signals at m/z 49 (methanethiol, protonated CH_4S), m/z 95 (dimethyl disulfide, protonated $C_2H_6S_2$), and m/z 127 (dimethyl trisulfide, protonated $C_2H_4S_3$). The maxima occur at different times: around 24 h, the first major peak corresponds to methanethiol (m/z 49), followed by increases in dimethyl disulfide (m/z 95) and dimethyl trisulfide (m/z 127). Subsequently, dimethyl disulfide shows a distinct profile, reaching a maximum at 96 h, when the methanethiol and dimethyl trisulfide signals have already decreased.

In the emissions recorded during the growth of *Agrococcus citreus* ($B_{Agr.cit.}$), an exponential temporal trend was observed for ammonia (**Figure II.4.12a,b**) and for hydrogen sulfide (**Figure II.4.12c**).

Investigating and interpreting profiles such as those shown in **Figure II.4.12-**performed for *A. citreus* as well as for the other identified/assigned species can provide major benefits for atmospheric chemistry studies from a kinetic–chemical perspective, particularly for atmospheric processes influenced by the presence of airborne microorganisms.

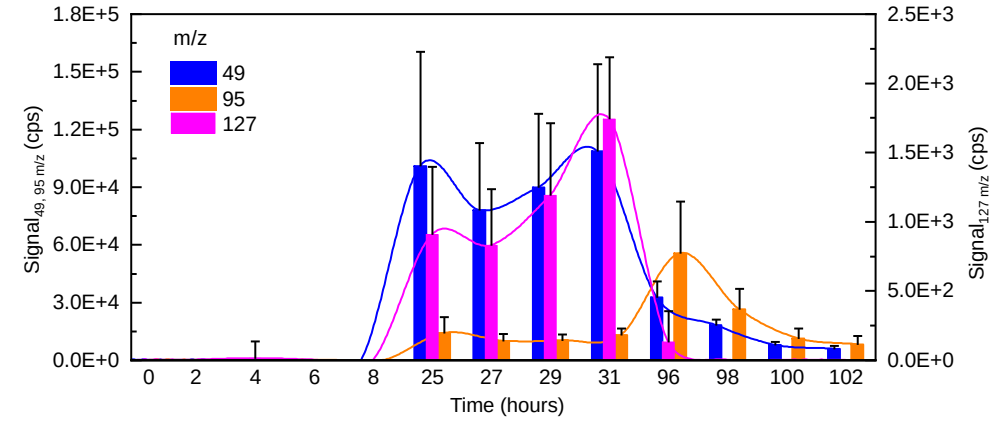

Figure II.4.11: Temporal variation profile of methanethiol (m/z 49), dimethyl disulfide (m/z 95), and dimethyl trisulfide (m/z 127) measured in the emissions of the bacterial isolate $B_{Pla.\ wig.}$.

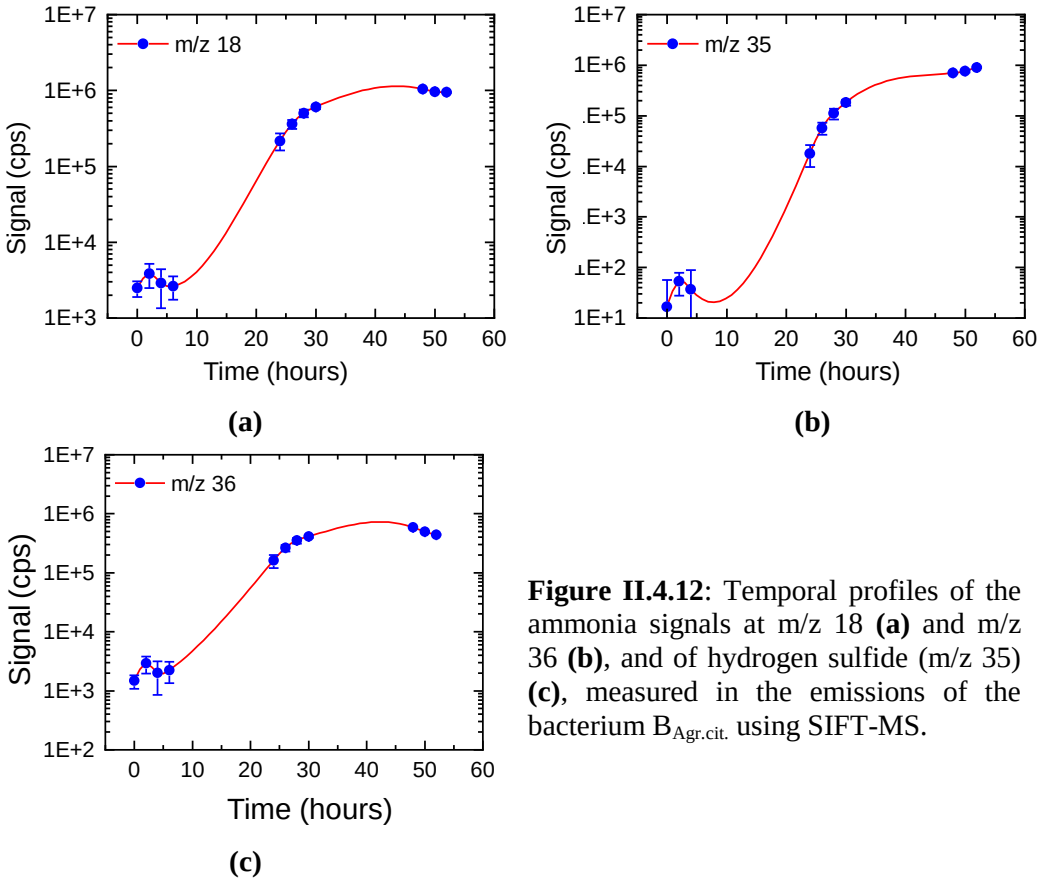

Figure II.4.12: Temporal profiles of the ammonia signals at m/z 18 **(a)** and m/z 36 **(b)**, and of hydrogen sulfide (m/z 35) **(c)**, measured in the emissions of the bacterium $B_{Agr.cit.}$ using SIFT-MS.

III FINAL CONCLUSIONS

Particulate matter (PM) and polycyclic aromatic hydrocarbons (PAHs): Active sampling proved reliable for size-segregated collection of PM fractions. $PM_{2.5}$ and PM_{10} concentrations frequently exceeded the limit values set by Directive (EU) 2024/2881, and PAH levels-particularly in winter-were elevated. The results indicate that fungal–bacterial interactions may play an essential role in the biogeochemical cycling of these compounds.

Microbiological characterisation: Passive sampling was suitable for assessing the microbiological load of ambient air. A complex diversity of microorganisms transported by air masses was documented: bacteria (*Planococcus wigleyi, Priestia aryabhattai, Agrococcus citreus, Arthrobacter* sp.), fungi (*Fusarium*, *Alternaria destruens*, *Alternaria* sp., *Cladosporium* sp.), and yeasts (*Aureobasidium* sp.). In bioaerosols associated with the airborne particulate matter fraction, both Gram-positive and Gram-negative bacteria with diverse morphologies-cocci, coccobacilli, and bacilli-were identified, together with fungal fragments (mycelia, hyphae) and spores (dictyospores and blastospores), indicating the coexistence of a diverse airborne community. The analyses suggest that *Alternaria destruens* may facilitate bacterial translocation in the presence of PAHs, and that yeasts of the genus *Aureobasidium* may contribute to the emission of volatile organic compounds (VOCs).

Molecular and elemental characterisation: The application of MALDI-Orbitrap MS and ICP-MS enabled elucidation of the chemical composition of bioaerosols. MALDI-Orbitrap MS facilitated the identification of bacterial membrane components (phosphatidylethanolamine, diacylglycerol) and specific metabolites (surfactin C and D), while isotopic evaluation was essential for confirming molecular formulae. MALDI–Orbitrap MS shows high potential for cellular and metabolic differentiation in studies of the molecular profile of atmospheric bioaerosols. ICP-MS revealed essential elements (Fe, Cu, Zn, Ni, Co, Mn, V), structural elements (Ca, Mg), as well as trace/ultra-trace elements (Al, B, Rb, Sr, Ba, Cr, Pb, Tl, Li, Cd, Bi, U). Fungi and yeasts exhibited higher tolerance than bacteria to the toxicity of elements such as U and Cd, supporting the hypothesis of their involvement in the biogeochemical cycling of toxic metals.

Analysis of volatile compounds (VOCs) emitted during microbial development: Using SIFT-MS, the active contribution of airborne microorganisms to atmospheric chemistry was demonstrated through the generation of atmospherically relevant compounds. Yeasts and bacteria emitted ammonia and hydrogen sulfide, whereas fungi showed acetone

emissions. SIFT-MS proved versatile for real-time monitoring of emission dynamics associated with microbial load in airborne bioaerosol fractions.

Over the course of the doctoral research, all five initial objectives were fully achieved, validating the experimental strategies. Optimised protocols were developed for active and passive sampling and for chemical characterisation of bioaerosols, integrated with UHPLC-FLD, MALDI-Orbitrap MS, and ICP-MS, and shown to be effective for investigating ambient particulate matter and its biological component.

Characterisation of urban PM in Iasi highlighted the seasonal variability of PAHs and potential emission sources, while also suggesting a role of fungal-bacterial interactions in biogeochemical processes. The microbiological component was documented for the first time in the region through identification of diverse bacteria, fungi, and yeasts in urban bioaerosols, with implications for public health and atmospheric dynamics.

At the molecular level, MALDI-Orbitrap MS and ICP-MS enabled the identification of peptide biomarkers, membrane components, and bacterial metabolites, as well as the determination of essential, structural, and trace/ultra-trace elements. Complementarily, SIFT-MS captured species-specific volatile emission profiles throughout microbial development, highlighting their contribution to atmospheric chemistry.

Overall, the objectives were met through quantitative measurements and advanced qualitative/molecular analyses, with internationally validated outcomes. This thesis strengthens current knowledge on bioaerosols associated with particulate matter in the urban area of Iasi and provides modern methodologies applicable to assessing environmental and public-health impacts.

Bibliography

Alberto, R.-F., Carlos, B.-A., Iris, A., Ana María, V.-M., Rosa María, V.-B., Chiara, S., Roberto, F., Ana Isabel, C., Paola, D. N., & Delia, F.-G. (2024, July 11). *Significance of emission sources identification for understanding the atmospheric load of Alternaria spores and Alt a 1 allergen.* https://doi.org/10.5194/egusphere-plinius18-77

Álvarez-Barragán, J., Cravo-Laureau, C., Xiong, B., Wick, L. Y., & Duran, R. (2023). Marine Fungi Select and Transport Aerobic and Anaerobic Bacterial Populations from Polycyclic Aromatic Hydrocarbon-Contaminated Sediments. MBio, 14(2). https://doi.org/10.1128/mbio.02761-22

Amarandei, C., Negru, A. G., Iancu, C., Olariu, R. I., & Arsene, C. (2024). Seasonality, sources apportionment, human health risks assessments, and potential implications on the atmospheric chemistry of polycyclic aromatic hydrocarbons in size-segregated aerosols from a Romanian metropolitan area. *Chemosphere*, *368*. https://doi.org/10.1016/j.chemosphere.2024.143738

Apangu, G. P., Frisk, C. A., Adams-Groom, B., Petch, G. M., Hanson, M., & Skjøth, C. A. (2023). Using qPCR and microscopy to assess the impact of

harvesting and weather conditions on the relationship between Alternaria alternata and Alternaria spp. Spores in rural and urban atmospheres. *International Journal of Biometeorology*, *67*(6), 1077–1093. https://doi.org/10.1007/s00484-023-02480-w

Arsene, C., Olariu, R. I., & Mihalopoulos, N. (2007). Chemical composition of rainwater in the northeastern Romania, Iasi region (2003–2006). *Atmospheric Environment*, *41*(40). https://doi.org/10.1016/j.atmosenv.2007.08.046

Arsene, C., Olariu, R. I., Zarmpas, P., Kanakidou, M., & Mihalopoulos, N. (2011). Ion composition of coarse and fine particles in Iasi, north-eastern Romania: Implications for aerosols chemistry in the area. *Atmospheric Environment*, *45*(4), 906–916. https://doi.org/10.1016/j.atmosenv.2010.11.013

Buiarelli, F., Sonego, E., Uccelletti, D., Bruni, E., Di Filippo, P., Pomata, D., Riccardi, C., Perrino, C., Marcovecchio, F., & Simonetti, G. (2019a). Determination of the main bioaerosol components using chemical markers by liquid chromatography–tandem mass spectrometry. *Microchemical Journal*, *149*, 103974. https://doi.org/10.1016/j.microc.2019.103974

Buiarelli, F., Sonego, E., Uccelletti, D., Bruni, E., Di Filippo, P., Pomata, D., Riccardi, C., Perrino, C., Marcovecchio, F., & Simonetti, G. (2019b). Determination of the main bioaerosol components using chemical markers by liquid chromatography–tandem mass spectrometry. *Microchemical Journal*, *149*, 103974. https://doi.org/10.1016/j.microc.2019.103974

Chakraborty, M., Sharma, B., Ghosh, A., Sah, D., & Rai, J. P. N. (2023). Elicitation of E-waste (acrylonitrile-butadiene styrene) enriched soil bioremediation and detoxification using Priestia aryabhattai MGP1. *Environmental Research*, *238*, 117126. https://doi.org/10.1016/j.envres.2023.117126

El Jaddaoui, I., Rangel, D. E. N., & Bennett, J. W. (2023). Fungal volatiles have physiological properties. *Fungal Biology*, *127*(7–8), 1231–1240. https://doi.org/10.1016/j.funbio.2023.03.005

Evtushenko, L. I., & Takeuchi, M. (2006). The Family Microbacteriaceae. In M. Dworkin, S. Falkow, E. Rosenberg, K.-H. Schleifer, & E. Stackebrandt (Eds.), *The Prokaryotes* (pp. 1020–1098). Springer New York. https://doi.org/10.1007/0-387-30743-5_43

Ferguson, R. M. W., Garcia-Alcega, S., Coulon, F., Dumbrell, A. J., Whitby, C., & Colbeck, I. (2019). Bioaerosol biomonitoring: Sampling optimization for molecular microbial ecology. *Molecular Ecology Resources*, *19*(3), 672–690. https://doi.org/10.1111/1755-0998.13002

Freiwald, A., & Sauer, S. (2009). Phylogenetic classification and identification of bacteria by mass spectrometry. *Nature Protocols*, *4*(5), 732–742. https://doi.org/10.1038/nprot.2009.37

Galon-Negru, A. G., Olariu, R. I., & Arsene, C. (2019). Size-resolved measurements of PM2.5 water-soluble elements in Iasi, north-eastern Romania: Seasonality, source apportionment and potential implications for human health. *Science of The Total Environment*, *695*, 133839. https://doi.org/10.1016/j.scitotenv.2019.133839

Grinn-Gofron, A. (2009). The occurrence of cladosporium spores in the air and their relationships with meteorological parameters. Acta Agrobotanica, 62(2), 111–116. https://doi.org/10.5586/aa.2009.032

Garcia-Alcega, S., Nasir, Z. A., Ferguson, R., Whitby, C., Dumbrell, A. J., Colbeck, I., Gomes, D., Tyrrel, S., & Coulon, F. (2017). Fingerprinting outdoor air environment using microbial volatile organic compounds (MVOCs) – A review. *TrAC Trends in Analytical Chemistry*, *86*, 75–83. https://doi.org/10.1016/j.trac.2016.10.010

Gollakota, A. R. K., Gautam, S., Santosh, M., Sudan, H. A., Gandhi, R., Sam Jebadurai, V., & Shu, C.-M. (2021). Bioaerosols: Characterization, pathways, sampling strategies, and challenges to geo-environment and health. *Gondwana Research*, *99*, 178–203. https://doi.org/10.1016/j.gr.2021.07.003

Guo, X., Xie, C., Wang, L., Li, Q., & Wang, Y. (2019). Biodegradation of persistent environmental pollutants by Arthrobacter sp. *Environmental Science and Pollution Research*, *26*(9), 8429–8443. https://doi.org/10.1007/s11356-019-04358-0

Gupta, R. S., Patel, S., Saini, N., & Chen, S. (2020). Robust demarcation of 17 distinct Bacillus species clades, proposed as novel Bacillaceae genera, by phylogenomics and comparative genomic analyses: Description of Robertmurraya kyonggiensis sp. nov. and proposal for an emended genus Bacillus limiting it only to the members of the Subtilis and Cereus clades of species. *International Journal of Systematic and Evolutionary Microbiology*, *70*(11), 5753–5798. https://doi.org/10.1099/ijsem.0.004475

Ha, M., Jo, H.-J., Choi, E.-K., Kim, Y., Kim, J., & Cho, H.-J. (2019). Reliable Identification of Bacillus cereus Group Species Using Low Mass Biomarkers by MALDI-TOF MS. *Journal of Microbiology and Biotechnology*, *29*(6), 887–896. https://doi.org/10.4014/jmb.1903.03033

Haig, C. W., Mackay, W. G., Walker, J. T., & Williams, C. (2016). Bioaerosol sampling: Sampling mechanisms, bioefficiency and field studies. *Journal of Hospital Infection*, *93*(3), 242–255. https://doi.org/10.1016/j.jhin.2016.03.017

Hanano, A., Moursel, N., & Obeid, M. H. (2025). Exploring the biodegradation activity of Priestia aryabhattai 1–3I, a promising chlorpyrifos-degrading strain isolated from a local phosphogypsum landfill. *Pesticide Biochemistry and Physiology*, *211*, 106416. https://doi.org/10.1016/j.pestbp.2025.106416

Ling, L., Luo, H., Yang, C., Wang, Y., Cheng, W., Pang, M., & Jiang, K. (2022). Volatile organic compounds produced by Bacillus velezensis L1 as a potential biocontrol agent against postharvest diseases of wolfberry. *Frontiers in Microbiology*, *13*, 987844. https://doi.org/10.3389/fmicb.2022.987844

Liu, Z., Zhang, Y., Fa, K., Zhao, H., Qin, S., Yan, R., & Wu, B. (2018). Desert soil bacteria deposit atmospheric carbon dioxide in carbonate precipitates. *CATENA*, *170*, 64–72. https://doi.org/10.1016/j.catena.2018.06.001

Manibusan, S., & Mainelis, G. (2022). Passive bioaerosol samplers: A complementary tool for bioaerosol research. A review. *Journal of Aerosol Science*, *163*, 105992. https://doi.org/10.1016/j.jaerosci.2022.105992

Manzulli, V., Rondinone, V., Buchicchio, A., Serrecchia, L., Cipolletta, D., Fasanella, A., Parisi, A., Difato, L., Iatarola, M., Aceti, A., Poppa, E., Tolve, F., Pace, L., Petruzzi, F., Rovere, I. D., Raele, D. A., Del Sambro, L., Giangrossi, L., & Galante, D. (2021). Discrimination of Bacillus cereus Group Members by MALDI-TOF Mass Spectrometry. *Microorganisms*, *9*(6), 1202. https://doi.org/10.3390/microorganisms9061202

Nithyashree, J. K., & Subramanian, S. (2025). Biomineralization Potential of Priestia aryabhattai, a Freshwater Isolate for Phosphorus Recovery through Struvite Production from Municipal Wastewater. Geomicrobiology Journal, 42(6), 507–522. https://doi.org/10.1080/01490451.2025.2477599

Pallen, M. J. (2024). Valid publication of names for bacterial species from the chicken gut. *International Journal of Systematic and Evolutionary Microbiology*, *74*(7). https://doi.org/10.1099/ijsem.0.006445

Pernil, R., & Schleiff, E. (2019). Metalloproteins in the Biology of Heterocysts. *Life*, *9*(2), 32. https://doi.org/10.3390/life9020032

Reese, K. L., Rasley, A., Avila, J. R., Jones, A. D., & Frank, M. (2020). Metabolic Profiling of Volatile Organic Compounds (VOCs) Emitted by the Pathogens Francisella tularensis and Bacillus anthracis in Liquid Culture. Scientific Reports, 10(1). https://doi.org/10.1038/s41598-020-66136-0

Rolph, G., Stein, A., & Stunder, B. (2017). Real-time Environmental Applications and Display sYstem: READY. *Environmental Modelling & Software*, *95*, 210–228. https://doi.org/10.1016/j.envsoft.2017.06.025

Roslund, K., Lehto, M., Pussinen, P., Groop, P.-H., Halonen, L., & Metsälä, M. (2020). On-line profiling of volatile compounds produced in vitro by pathogenic oral bacteria. *Journal of Breath Research*, *14*(1), 016010. https://doi.org/10.1088/1752-7163/ab5559

Silvestri, E. (2014). *Evaluation of Options for Interpreting Environmental Microbiology Field Data Results having Low Spore Counts*. EPA 600/R-14/331, U.S. Environmental Protection Agency.

Sindt, C., Besancenot, J.-P., & Thibaudon, M. (2016). Airborne Cladosporium fungal spores and climate change in France. Aerobiologia, 32(1), 53–68. https://doi.org/10.1007/s10453-016-9422-x

Stein, A. F., Draxler, R. R., Rolph, G. D., Stunder, B. J. B., Cohen, M. D., & Ngan, F. (2015). NOAA's HYSPLIT Atmospheric Transport and Dispersion Modeling System. *Bulletin of the American Meteorological Society*, *96*(12), 2059–2077. https://doi.org/10.1175/BAMS-D-14-00110.1

Uddin, S., Habibi, N., Fowler, S. W., Behbehani, M., Gevao, B., Faizuddin, M., & Gorgun, A. U. (2023). Aerosols as Vectors for Contaminants: A Perspective Based on Outdoor Aerosol Data from Kuwait. *Atmosphere*, *14*(3), 470. https://doi.org/10.3390/atmos14030470

Xue, F., Yang, Y., Lai, S., Xiao, Y., Yao, Y., Zhang, Y., & Zou, S. (2023). Airborne microbiomes at a subtropical island in southern China: Importance of the northwest and southeast monsoons. *Atmospheric Environment*, *307*, 119842. https://doi.org/10.1016/j.atmosenv.2023.119842

Zhang, R., Zhang, Y., Zhang, T., Xu, M., Wang, H., Zhang, S., Zhang, T., Zhou, W., & Shi, G. (2022). Establishing a MALDI-TOF-TOF-MS method for rapid identification of three common Gram-positive bacteria (Bacillus cereus, Listeria monocytogenes, and Micrococcus luteus) associated with foodborne diseases. *Food Science and Technology*, *42*, e117021. https://doi.org/10.1590/fst.117021

List of original contributions presented in this doctoral thesis

Full-length scientific articles published in peer-reviewed journals indexed in Web of Science and Scopus, with an impact factor.

Amarandei, C., Negru, A.G., **Iancu, C.**, Olariu, R. I., Arsene, C. Seasonality, sources Apportionment, human health risks assessments, and potential implications on the atmospheric chemistry of polycyclic aromatic hydrocarbons in size-segregated aerosols from a Romanian metropolitan area. *Chemosphere*, 368, **2024**.
https://doi.org/10.1016/j.chemosphere.2024.143738

Impact factor: **8.10 -** Q1 quartile (red zone).

Iancu, C., Nita, C., Soroaga, L.V., Negru, A.G., Olariu, R.I., Arsene, C. First chemical insights into airborne microbial communities isolated from ambient particulate matter in the Iasi urban area, north-eastern Romania. Journal of Liquid Chromatography and Related Technologies, **2025**. https://doi.org/10.1080/10826076.2025.2554062

Impact factor: **1.20 –** Q4 quartile (white zone).

Participation in conferences and scientific events

șOral presentations

Iancu, C., Soroaga, V.L., Negru, A.G., Olariu, R.I., Arsene, C., Elemental composition of bacteria, fungi, and yeasts isolates from airborne bioaerosol particles, The 16th Scientific Session of Undergraduate, Master and PhD Students, Iasi, Romania, Book of Abstracts, p. 18, oral presentation, 19 June, **2025**.

Iancu, C., Nita, C., Negru, A.G., Soroaga, L.V., Olariu, R.I., Arsene, C., Research tools for the investigation of bacteria land fungal communities in bioaerosol particles, Recent Advances in Natural Sciences Yield the Future for the European Citizens and Society, Ready for Europe Conference - RARE 2024, 1st Edition, Iasi, Romania, Book of Abstracts, p. 17, oral presentation, 12-13 December, **2024**.

Amarandei, C., **Iancu, C.**, Negru, A.G., Soroaga, L.V., Olariu, R.I., Arsene, C., Real-time analysis of gases at trace levels with selected ion flow tube mass spectrometry (SIFT-MS) technology, Recent Advances in Natural Sciences Yield the Future for the European Citizens and Society, Ready for Europe Conference - RARE 2024, 1st Edition, Iasi, Romania, Book of Abstracts, p. 47, oral presentation, 12-13 December, **2024**.

Iancu, C., Mihalache, G., Amarandei, C., Negru, A.G., Grădinaru, R., Costică, N., Bejan, I.G., Olariu, R.I., Arsene, C., First insights into atmospheric bioaerosols from the Iasi urban area, The 13th Scientific Session of Undergraduate, Master and PhD Students, Iasi, Romania, Book of Abstracts, p. 24, oral presentation, 28 October, **2022**.

Posters

Iancu, C., Amarandei, C., Negru, A.G., Olariu, R.I., Arsene, C., Selected ion flow tube mass spectrometry investigation of volatile compounds emitted by microorganisms of atmospheric origin, IasiCHEM 2024 Conference, 6th Edition,

Iasi, Romania, Book of Abstracts, p. 45, poster, 31 October - 01 November, **2024**.

Amarandei, C., Negru, A.G., **Iancu, C.**, Olariu, R.I., Arsene, C., Analysis of size-segregated particle-bound polycyclic aromatic hydrocarbons in Iasi urban area, National Conference of Chemistry, XXXVII Edition, Targoviste, Romania, Book of Abstracts, poster, 25-27 September, **2024**.

Iancu, C., Amarandei, C., Costica, N., Bejan, I.G., Olariu, R.I., Arsene, C., Microscopic and molecular approaches into atmospheric bioaerosols from the Iasi urban area, IasiCHEM 2023 Conference, 5th Edition, Iasi, Romania, Book of Abstracts, p. 31, poster, 26-27 October, **2023**.